KTH ROYAL INSTITUTE
OF TECHNOLOGY

Doctoral Thesis in Fibre and Polymer Science

Protected Lignin Biorefining: Fundamental Insights on Lignin Reactivity

MARIA KARLSSON

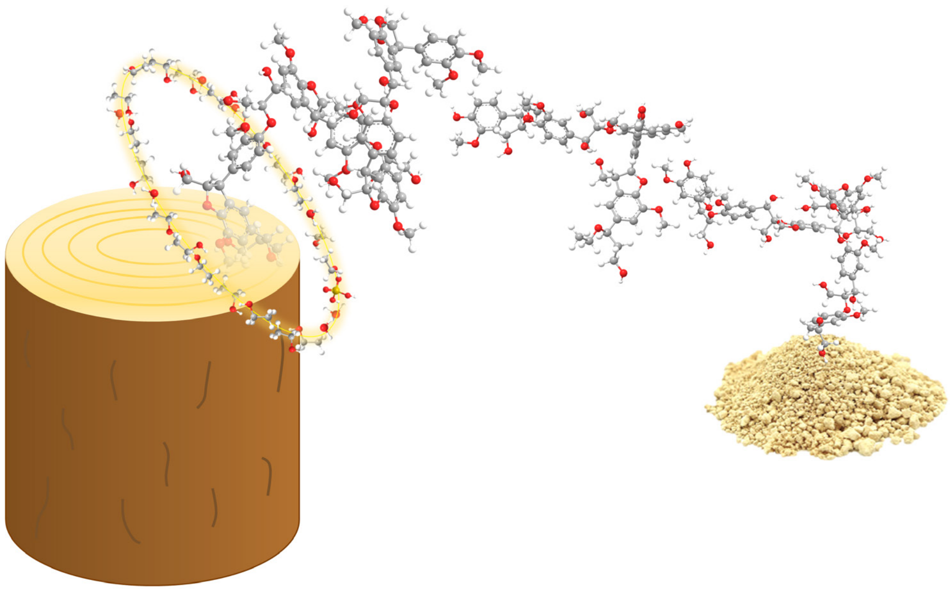

Stockholm, Sweden 2023

Protected Lignin Biorefining: Fundamental Insights on Lignin Reactivity

MARIA KARLSSON

Academic Dissertation which, with due permission of the KTH Royal Institute of Technology, is submitted for public defence for the Degree of Doctor of Philosophy on Friday the 2nd June 2023, at 10:00 a.m. in F3, Lindstedtsvägen 26, Stockholm.

Doctoral Thesis in Fibre and Polymer Science
KTH Royal Institute of Technology
Stockholm, Sweden 2023

ISBN: 978-91-8040-564-5
TRITA-CBH-FOU-2023:18

Printed by: Universitetsservice US-AB, Sweden 2023

Abstract

The potential to utilize lignin, which constitutes as much as 15-30% of the biomass, needs further evaluation. In the transition towards a bioeconomy, lignin has the potential to replace fossil-based phenols. Attempts to valorize the available technical lignins are ongoing; however, that lignin suffers from molecular heterogeneity. Accordingly, new process concepts, coined in the term lignin biorefineries, are required to obtain less heterogenic lignin with different properties and preserved molecular structure.

In this study, a new lignin extraction concept was investigated, where the structural properties of lignin were preserved to a high degree using a physical protection strategy. The principle of preserving the lignin structure was based on a cyclic organosolv extraction concept. At first, a two-step concept was evaluated, where a hydrothermal extraction was performed to recover hemicellulose, followed by a cyclic organosolv extraction to obtain the lignin. Trend studies were performed for the individual cycles to gain a deeper understanding of how the lignin structure was affected by the cycles. To further investigate the method, chemometrics and design of experiment were used to gain knowledge about how different properties of lignin were affected by the extraction conditions and how the properties of lignin could be tailored. Based on the knowledge from the chemometric study and the observations from the two-step method, a refined one-step method was developed to obtain lignin with further improved analytical quality, i.e., up to 95% of the interunit linkages could be assigned for spruce lignin by heteronuclear single quantum coherence (HSQC) nuclear magnetic resonance (NMR) spectroscopy, ^{13}C NMR and size exclusion chromatography (SEC). The universality of the method was investigated for different wood species, such as spruce and birch. The results indicate the applicability of the concept using different raw materials.

The complex nature of lignin substrates conveys the need for robust analytic techniques. Herein, NMR studies were complemented by matrix-assisted laser desorption/ionization (MALDI) time of flight (TOF) mass spectrometry (MS) to provide new insights into molecular lignin populations with respect to reactivity during the organosolv extraction.

Finally, a proof of concept for an application was investigated. The cyclic organosolv extracted lignin was used in a fundamental study on lignin nanoparticles (LNP), together with benchmark technical lignins, to gain knowledge about the role of the molecular structure in the LNP properties. It is suggested that the molecular structure of lignin plays an important role in determining the size and morphology of LNPs, opening possibilities to molecularly tailor LNP properties.

Keywords

Sustainability, lignin, biorefinery, cyclic organosolv extraction, preserved structure, NMR, MALDI-TOF MS.

Sammanfattning

Potentialen av att använda lignin, som utgör 15-30% av biomassan, behöver utvärderas ytterligare. I övergången till en bioekonomi finns potential för lignin att ersätta fossila fenoler. I denna kontext försöker man hitta ett värde för de tillgängliga tekniska ligninerna, men det finns utmaningar associerade med den molekylära strukturella heterogeniteten. Följaktligen behövs nya processkoncept, såsom lignin-bioraffinaderier, där man kan ta fram ett lignin med olika önskade egenskaper samt med en bevarad molekylstruktur.

I denna studie utvecklades ett nytt koncept för att extrahera lignin, där ligninets strukturella egenskaper kunde bevaras i hög grad med hjälp av en fysisk skyddsstrategi. Principerna för att bevara ligninstrukturen baserades på ett cykliskt organosolv-extraktions-koncept. Först utvärderades en två-stegs koncept, där en hydrotermisk extraktion, för att extrahera ut hemicellulosa, efterföljdes av en cyklisk organosolv-extraktion för att extrahera ut lignin. Trendstudier utfördes för de individuella cyklerna för att få en fördjupad förståelse av hur ligninstrukturen påverkades av cyklerna. För att ytterligare undersöka metoden användes kemometri och experimentell design för att öka kunskapen om hur olika extraktionsförhållanden påverkade egenskaper hos ligninet samt hur egenskaperna hos ligninet kunde skräddarsys. Genom den erhållna kunskapen från den kemometriska studien och den studerade trenden av två-stegsmetoden, undersöktes en kortare en-stegs metod för att kunna erhålla ett lignin med ytterligare förbättrad analytisk kvalité, där upp till 95% av bindningarna kunde bestämmas för granlignin, karaktäriserat med *heteronuclear single quantum coherence* (HSQC) *nuclear magnetic resonance spectroscopy* (NMR), ^{13}C NMR och *size exclusion chromatography* (SEC). Metodens universalitet undersöktes för träslag med olika lignin-egenskaper som gran och björk. Resultaten indikerade tillämpbarheten av konceptet för olika råvaror.

På grund av den komplexa naturen hos lignin finns ett behov av robusta analystekniker. För att möta detta kompletterades NMR-studier med *matrix-assisted laser desorption/ionization* (MALDI) *time of flight* (TOF) *mass spectrometry* (MS) analyser för att få nya insikter om olika molekylära ligninpopulationer samt för att öka kunskapen om ligninreaktiviteten under organosolv-extraktion.

Slutligen gjordes en undersökning av hur det cykliska ligninet förhöll sig mot en applikation. Det cykliska organosolv-extraherade ligninet användes i en fundamental studie om lignin-nano partiklar (LNP), tillsammans med benchmark-tekniska ligniner, för att öka insikter om de molekylära egenskapernas roll för LNP-egenskaperna. Det har visat sig att den molekylära strukturen spelar en betydande roll för att bestämma storleken och morfologin hos LNP, vilket öppnar upp för möjligheter att molekylärt skräddarsy LNP-egenskaper.

Nyckelord

Hållbarhet, lignin, bioraffinaderi, cyklisk organosolv extraktion, bevarad struktur, NMR, MALDI-TOF MS.

List of papers

This thesis is based on the following papers:

I. **Toward a Consolidated Lignin Biorefinery: Preserving the Lignin Structure through Additive-Free Protection Strategies**
M. Karlsson, N. Giummarella, P. A. Linden, M. Lawoko
ChemSusChem, 2020, 13, 4666-4677

II. **Protected lignin biorefining through cyclic extraction: gaining fundamental insights into the tuneable properties of lignin by chemometrics**
M. Karlsson, V. L. Vegunta, R. Deshpande, M. Lawoko
Green Chemistry, 2022, 24, 1211-1223

III. **A Flexible Physical Protection Process for Lignin Extraction**
M. Karlsson, M. Lawoko
Submitted

IV. **Lignin Structure and Reactivity in Organosolv process Studied by NMR Spectroscopy, Mass Spectrometry and Density Functional Theory**
M. Karlsson, J. Romson, T. Elder, Å. Emmer, M. Lawoko
Biomacromolecules, DOI: 10.1021/acs.biomac.3c00186

V. **Molecular understanding of the morphology and properties of lignin nanoparticles: Unravelling the potential for tailored applications**
I. V. Pylypchuk*, M. Karlsson*, P. A. Lindén, M. Lindström, T. Elder, O. Sevastyanova, M. Lawoko
Submitted
*equal contribution

Author's contribution to the appended papers:

I. First author. Project planning, performed most of the experimental work, interpreted results, and wrote the original draft.

II. First author. Project planning, performed most of the experimental work, interpreted results, and wrote a major part of the original draft.

III. First author. Project planning, all experimental work, interpreted results and wrote the original draft.

IV. First author. Project planning, performed most of the experimental work, interpreted results, and wrote the original draft.

V. Shared first author. Performed part of the experimental work (all experiments related to the crude lignin), interpreted results, and wrote the original draft with co-authors.

Author's conference presentations:

ACS Spring 2021 National Meeting & Exposition, 2021, 5^{th}-30^{th} April, online
Integrated lignin biorefinery: Preserving the lignin structure through additive-free protection strategies
Oral presentation

Treesearch Progress Conference, 2022, 11^{th}-12^{th} May, Norrköping, Sweden
Bark biorefinery; fundamental insights on the properties of a novel organosolv lignin from Norway spruce bark
Oral presentation

CA17128 LignoCOST Lignin Conference, 2022, 31^{st} May-3^{rd} June, Wageningen, Netherlands
Correlation between the molecular structure of lignin and the properties of its nanoparticles, using lignin from different processes
Oral presentation

16th European Workshop on Lignocellulosics and Pulp (EWLP), 2022, 22^{nd}-26^{th} June, Gothenburg, Sweden
Consolidated lignin biorefinery using a physical protection strategy to preserve the lignin structure
Oral presentation

MWP Young Researchers' Program, 2022, 9^{th}-11^{th} October, Stockholm, Sweden
Toward new process design: Preserving the lignin structure by using a physical protection strategy
3 min pitch and poster presentation

Papers not included in this thesis

I. **Fundamental Insights on the Physical and Chemical Properties of Organosolv Lignin from Norway Spruce Bark**
B. Rietzler, M. Karlsson, I. Kwan, M. Lawoko and M. Ek
Biomacromolecules, 2022, 23, 3349-3358

Abbreviations

Alcell	alcohol cellulose
Ar	aromatic units
ASE	accelerator solvent extractor
β-5′	phenylcoumaran
β-β′	resinol
β-O-4′	β-aryl ether
CA	coumaryl aldehyde
CA-OH	coniferyl alcohol
Đ	dispersity
Da	dalton
DBDO	dibenzodioxocin
DFT	density functional theory
DHB	2,5-dihydroxybenzoic acid
DMSO	dimethyl sulfoxide
DoE	design of experiment
DP_n	degree of polymerization
EtOH	ethanol
G	guaiacyl
H	*p*-hydroxyphenyl
HK	Hibbert's ketone
HPAEC	high-performance anion-exchange chromatography
HPLC	high-performance liquid chromatography
HSQC	heteronuclear single quantum coherence
HW	hardwood
LCC	lignin carbohydrate complex
LNPs	lignin nanoparticles
m/z	mass-to-charge ratio
M_n	number average molecular weight
M_w	weight average molecular weight
MALDI	matrix-assisted laser desorption/ionization
MLR	multiple linear regression
MS	mass spectrometry
MWL	milled wood lignin
NMR	nuclear magnetic resonance spectroscopy
OS	organosolv
PAD	pulsed amperometric detector
RI	refractive index

S	syringyl
SDGs	sustainable development goals
SEC	size exclusion chromatography
SW	softwood
THF	tetrahydrofuran
TOF	time of flight
UV	ultraviolet

Contents

1 Introduction

1.1 Lignin

Lignin is the most abundant aromatic polymer in nature, accounting for 15-30% of the biomass, depending on the species. [1-3] Lignin is deposited with the hemicellulose between the cellulose microfibrils and contributes to the strength and rigidity of the cell wall. Lignin also protects against microbial attacks and assists in water transport in plants due to its hydrophobic properties. [4, 5]

Lignin is a racemic heteropolymer with a multifunctional structure still under investigation [6-8]. The main monolignols (lignin monomers) forming the polymer are illustrated in Figure 1. Lignin-containing biomass includes softwood (SW) and hardwood (HW). SW lignin, such as spruce lignin, mainly consists of guaiacyl (G) units formed by coniferyl alcohol coupling, with trace amounts *p*-hydroxyphenyl (H), formed by the coupling of *p*-coumaryl alcohol. HW lignin, such as birch lignin, consists mainly of syringyl (S) and G units with trace amounts of H units. Grass lignin consists of S, G and H units, where the content of H units is higher than for SW and HW lignin. [9] Lignin is incorporated in the cell wall layers and middle lamella [4]. The lignin content varies between species, parts of the plant, and cell wall layers. The secondary cell wall contains the main part of lignin due to the large relative volume, even though the lignin concentration is higher in the middle lamella [10, 11].

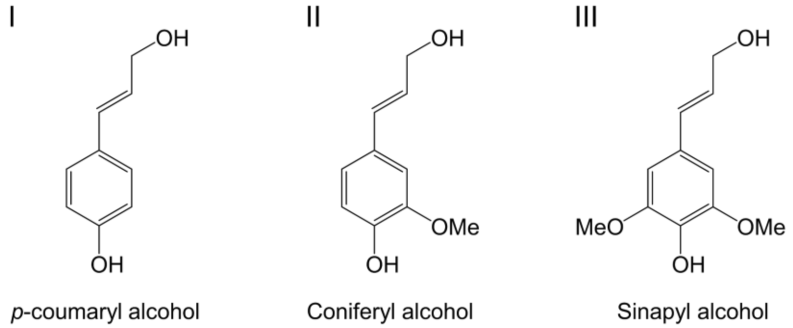

Figure 1. The main monolignols in lignin, where the *p*-coumaryl alcohol (I) forms H units, coniferyl alcohol (II) forms G units, and sinapyl alcohol (III) forms S units in the lignin polymer.

The monolignols are linked by ether and carbon-carbon bonds. The polymerization occurs by radical coupling reactions illustrated in Figure 2, specified for the β-aryl ether (β-O-4′), resinol (β-β′), and phenylcoumaran (β-5′) interunit linkages. An endwise polymerization is suggested rather than a bulk polymerization for the growing polymer [12]. The mechanism of the formation of dimers and oligomers starts with the oxidation of monolignols to radicals with different possible resonance forms, which act as building blocks in further polymerization Figure 2 (I). The dimeric β-O-4′ interunit linkage is formed by the radical coupling of the β-radical and a phenoxy radical to form the quinone methide intermediate. Subsequently, the addition of water to the quinone methide hydroxylates the α-position (II). The β-β′ interunit linkage is formed by the radical coupling of two β radicals (III). This is followed by an internal trapping reaction of the quinone methide intermediate by proximate hydroxyl groups to yield a pinoresinol structure. Similarly, the β-5′ interunit linkage is formed by the radical coupling of a β-radical and an Ar-5 radical, followed by the trapping reaction of the quinone methide and the phenol on the adjacent monolignol (IV) [13]. These reactions are followed by re-aromatization.

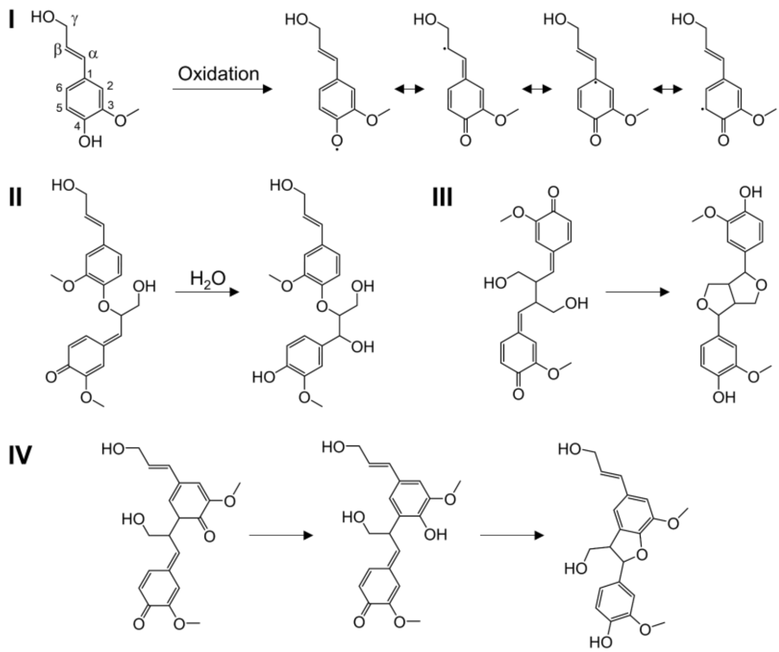

Figure 2. Lignin polymerization by oxidation of the monolignol and the subsequently formed radicals (I) involved in the formation of the dimers: β-O-4′ (II), β-β′ (III), and β-5′ (IV). The radical coupling of β- and phenoxy radicals form the dimeric β-O-4′ interunit linkage (II). The β-β′ interunit linkage (III) is formed through the radical coupling of two β-radical quinone methide intermediates followed by a trapping reaction between the quinone methide intermediates and hydroxyls located at the γ-position on the monolignols. The β-5′ interunit linkage (IV) is formed by the radical coupling of β- and Ar-5 radicals followed by a trapping reaction between the α-position of the quinone methide intermediate and the phenol.

The dominant type of inter-monomer linkage for lignin in wood is the β-O-4′ ether linkage [8], and the content may vary between wood species. For instance, the content of native β-O-4′ linkages in spruce lignin is around 60% and around 80% in birch lignin [6]. Native lignin properties remain a topic for deeper investigations due to the challenges with extracting it in unmodified form for detailed characterization. The properties include polarities, structural configuration, and inter- and intra-molecular interactions, such as hydrogen bonding and π-π interactions [14]. Based on model studies, a more linear lignin structure has been proposed [6]. From another viewpoint, a more branched model has been suggested based on an analysis of milled wood lignin (MWL) from spruce [7].

Covalent interactions between the biomass polymers have also been proposed, and constitute what is termed lignin carbohydrate complex (LCC). The proposed linkages between the lignin and carbohydrate moieties are phenyl glycosides, ether, or ester bonds [15]. Interactions between lignin and cellulose microfibrils have also been suggested [16, 17].

Given the complex nature of the lignin macromolecule and the complex interactions with other cell wall polymers, the chemical properties of lignin remain under investigation and will benefit from deeper characterization at the molecular scale. Such investigations will inform future biorefinery and valorization efforts.

1.2 Organosolv lignin extraction

A process that never attained large-scale industrial production of pulp was the organosolv (OS) process. The OS process was patented by Kleinert in the 1970s but had been investigated earlier for the isolation of wood components [18, 19]. Different solvents have been used for the delignification, such as alcohols, dioxane, and acetone. The delignification is often performed at high temperatures causing high pressure, in the range of 10-30 bar. [19] A promising OS-based solvent system for the delignification is aqueous-ethanol, which was investigated for small-scale plants [20]. The “alcohol cellulose” (Alcell) process, based on an aqueous-ethanol solvent system, was developed by the Canadian pulp and paper industry [21], and the first demonstration mill was completed in 1989 [22]. The lignin extraction is generally performed at a temperature between 160°C and 220°C using 20 wt% to 80 wt% of ethanol in an aqueous-ethanol solvent in a batch extraction [23]. Due to the relatively low boiling point of ethanol, it can be recovered by distillation [21, 24]. The fibers are recovered in the solid phase, and the dissolved lignin and carbohydrates, such as hemicelluloses in the effluent. Highly valuable products such as pulp, furfural, acetic acid, and lignin could be retrieved from the lignocellulosic biomass processed by the Alcell process [22].

The delignification can be performed with or without catalysts and additives [20, 25]. Commonly, mineral acid is added as catalyst [26]. When the process is performed without adding an acid, a lowering in pH occurs due to the hydrolysis and deacetylation with the formation of acetic acid from the hemicellulose. Apart from enhancing the delignification, performing the process under acidic conditions causes acidolysis of ether bonds in lignin and lignin-carbohydrate bonds in LCCs. Due to the nature of the products formed from the acidolysis, subsequent formation of high molecular weight lignin due to condensation reactions may occur. Furthermore, the formation of pseudo lignin derived from hemicellulose has been reported. [22] It is suggested that the condensation reactions cause recalcitrance and slower delignification. As these condensation reactions mainly occur between aromatic nuclei and electrophilic sites created on the aliphatic side chains, the nature of monolignols in lignin is important. For instance, due to the structural feature of SW lignin, which mainly consists of G units, the degree of condensations is higher than for HW lignin which additionally contains S units. This is because the second, fifth, and sixth positions on the aromatic G-ring are available for the electrophilic attack by the carbocation formed at the aliphatic side-chain causing stable carbon-carbon bonds. The aromatic S-rings only have the second and sixth positions available for such reactions[24].

Under acidic OS process conditions, depolymerization through acidolysis of β-O-4′ interunit and condensation reactions between the formed electrophilic benzylic cation and the electron-rich sites on the aromatic carbons occurs [27]. The β-O-4′ moieties have several pathways that are specifically illustrated for SW lignin in Figure 3. In the first step, an α-carbocation is formed stepwise by protonation of the hydroxyl group on the α-position and the subsequent release of water, Figure 3. One of the major depolymerization routes is the reaction of β-O-4′ interunit leading to the formation of ketones such as Hibbert's ketone [28-30], Figure 3 (I). The mechanistic route for the formation of Hibbert's ketone has been investigated [30, 31]. Repolymerization through inter and- intramolecular condensation reactions is illustrated in Figure 3. A phenylcoumaran-like structure formed through an α-5′ intramolecular condensation (II) has been reported [32]. By similar principles, the intermolecular α-5′ condensation (III) can be formed through the substitution reaction of the benzylic cation on C_α and the nucleophilic C5 carbon on another lignin molecule. The intermolecular α-5′ condensation could cause recalcitrance due to the effects of increased molecular weight. The proposed mechanism for the intermolecular 5-5′ condensation (IV) is somewhat different. Initially, homolytic cleavage of the β-O-4′ linkage forms β- and phenoxy radicals, Figure 4. The resonance 5-radicals couple to form stable 5-5′ structures. The formation of α-6′ condensations (V) is suggested to follow a similar mechanistic route as for the formation of intermolecular α-5′

condensation (III). The nucleophilic addition of the solvent, i.e., ethanol, to form the etherified capping on C_α (VI) is reported for Alcell-derived lignin [32]. The etherification prevents condensation at the C_α position.

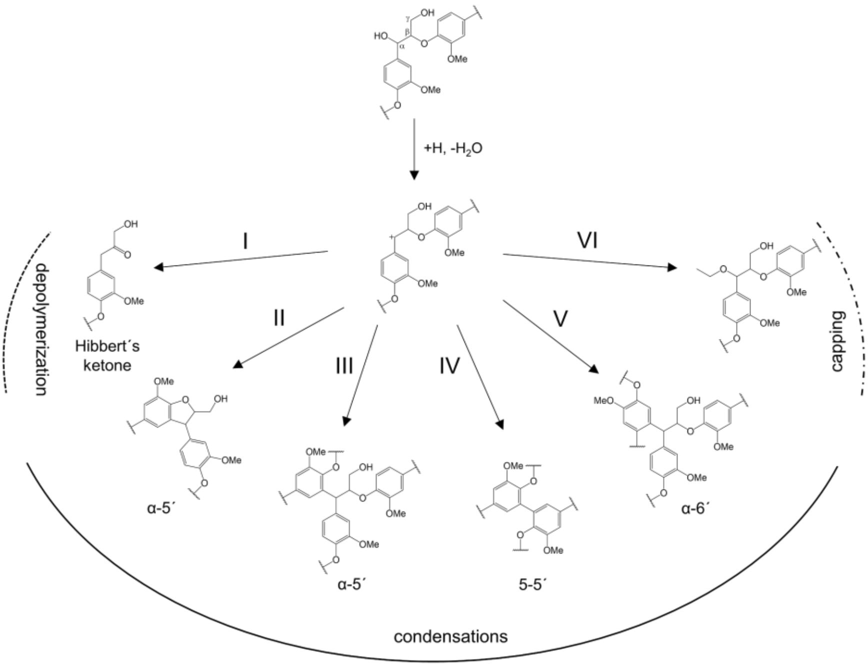

Figure 3. Pathways for a β-O-4′ unit at acidic aqueous-ethanol based OS Alcell extraction. The formation of benzylic cation, Hibbert's ketone (I), α-5′ intramolecular condensation (II), α-5′ intermolecular condensation (III), 5-5′ condensation (IV), α-6′ condensation (V) and etherification on C_α (VI).

Studies have been performed to increase the understanding of the acidolysis mechanisms for the β-O-4′ cleavages. Homolytic cleavages of the β-O-4′ interunit have been proposed, where the mechanism is based on the formation of quinone intermediates and β- and phenoxy radicals, Figure 4 [33, 34]. A correlation between temperature and the occurrence of homolytic cleavages has been proposed, with an increase of cleavage products at a higher temperature, starting from 130 °C [34].

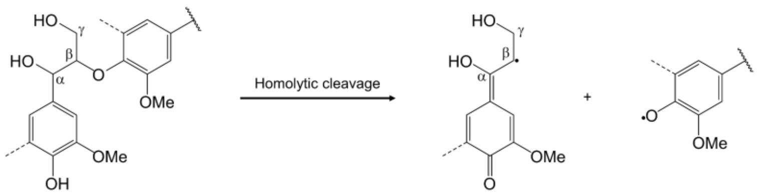

Figure 4. Homolytic cleavage of β-O-4′ under acidolysis, with the formation of quinone methide intermediate and reactive radicals, illustrated for both SW (G) and HW (S).

Another study challenged the commonly reported homolytic cleavage of β-O-4′ motifs, instead suggesting heterolytic cleavage through an unzipping mechanism from the phenolic ends. [35] Hence, further investigations might be necessary to define reaction mechanistic routes. Enol ether structures are not commonly reported for OS lignin but might form [27] through the elimination of formaldehyde.

Overall, at organosolv acid extraction conditions, a heterogenic reacted lignin with complex structure is obtained through depolymerization and repolymerization reactions, with extensive hydrolysis of the β-O-4′ interunit linkages. The amount of preserved native linkages is low and correlates well with the severity of the process [36-40]. The poor knowledge of the structure, due to the heterogeneity of the retrieved lignin, is not only observed for lignin obtained from the OS Alcell process but also from the largest technical pulping process today, the kraft process, which features a similar challenge [41-43].

Different strategies based on chemical and physical protection strategies have been proposed to prevent undesired reactions and degradation of lignin during extraction [44]. The principle of using chemical protection is to deactivate reactive sites that could cause degradation and condensation by using chemical additives. By deactivating the electrophilic carbocations on the aliphatic side-chains formed under acidic conditions, condensations can be prevented. For instance, the OS-based aldehyde-assisted fractionation process applies a chemical protection strategy. Here, aldehydes are added to prevent the formation of the benzylic cation on the lignin polymer through acetalization, thereby preventing the formation of stable carbon-carbon bonds in lignin. [45-47] Similar principles using acetalization to prevent further condensations have been adopted for acidolysis lignin, where ethylene glycol was used to stabilize reactive intermediates by forming acetal structures [48, 49]. Another strategy to reduce the alteration of the lignin structure is by using physical protection strategies such as a flow-through extraction method [44]. A continuous extraction, using the flow-through principle, has successfully been applied to obtain lignin with preserved β-O-4′ interunit linkages, which might be suitable for depolymerization and monomer production due to the high content of ether bonds [50-54]. The high content of β-O-4′ is often a good indicator for the preservation of the native structure since such bonds are more sensitive to reactions than carbon-carbon bonds.

1.2.1 Biorefinery processes

A common definition of biorefinery is the extraction of sustainable materials from biomass for conversion into marketable materials and energy, equivalent to a petroleum refinery [55-57]. Biorefinery processes and related concepts have captured interest due to the need to reduce the dependence on petrol-based resources. In this context, components from biomass can be converted to different chemicals, biomaterials, and bioenergy, consequently contributing to a more sustainable society and circular economy. In addition, depending on the synthesis strategies, biobased products have the potential to be recycled and used in several cycles, which is advantageous for both resource circularity and from a sustainable perspective. [55]

1.3 Sustainability

In 2015, the UN released the 17 UN Sustainable Development Goals (SDGs) aimed at abating poverty in society, addressing environmental concerns, and promoting sustainable economic and social practices. [58] There are 3 of the 17 SDGs that have been primarily the focus within this thesis; goal number 9 (industry, innovation and infrastructure), number 12 (responsible consumption and production), and number 13 (climate action). Generally, in transitioning from a fossil-based society to a biobased one, there is a need to find suitable precursor substitutes from biomass. Biomass is a renewable and sustainable resource on earth and has the potential as an alternative to fossil sources. [59] In this context, a new process concept to obtain high-quality raw materials for further valorization is of interest. This also involves the use of unutilized or under-utilized resources such as industrial by-products. The contribution of this thesis to the SDGs is to build profound knowledge of the lignin properties and use such knowledge to design process concepts that target a high value of several parts of the biomass, including lignin. Examples of how the SDGs connect to the research are listed below, where the developed method for lignin extraction addresses;

a) goal number 9 “Industry, innovation and infrastructure”: an innovative concept of obtaining high-quality lignin with preserved structure has been developed.

b) goal number 12 “Responsible production and consumption”: a unique lignin product with well-characterized properties is obtained. This opens the door for further valorization to biomaterials and biochemicals, as opposed to fossil-based products.

c) goal number 13 “Climate action”: the process uses green chemicals, and emissions are minimized due to the easy recovery of the solvents (ethanol and water) by low-temperature distillation. Besides, the process is potentially circular since the solvent can be produced from the other streams, i.e., fiber fraction. Furthermore, under-utilized biomass, specifically saw meal, has been utilized to retrieve the lignin. This is traditionally burnt, causing carbon dioxide emissions. The utilization here also addresses goal number 12 on responsible production and consumption.

1.4 The aim and objectives of the study

The aim of the study was to build a deeper knowledge basis on how lignin is affected by extraction and how the lignin structure can be preserved and tailored in new process concepts. Two important criteria considered were process sustainability and flexibility. To fulfill this aim, one objective was to investigate the possibility of an additive-free physical protection process concept to retrieve less complex lignin with preserved integrity. Benchmarks lignin produced using traditional delignification conditions would then be used as comparative references to assess product qualities. To investigate possibilities to tailor lignin structure, chemometric studies were used to relate extraction conditions with lignin properties. For process sustainability, green solvents with low boiling points were used. This consideration targets low-temperature solvent recovery by distillation. The process flexibility was addressed by studying process efficiency in different wood species and by studying the effects on lignin properties with and without a presiding hydrothermal extraction step. Finally, to obtain a deeper knowledge of the studied lignin samples, robust analytic techniques were required, and the strategy adopted was to use techniques that would complement each other. These techniques included several NMR methods, SEC and MALDI-TOF MS.

2 Material and Methods

A brief description of the material and methods related to the discussions in this thesis are given in this section. More detailed descriptions of the material and methods can be found in the appended papers I to V.

2.1 Lignin extraction

Wood from Norway spruce and birch was used as raw materials. The wood was milled (Wiley mini mill, 3383-L70, Thomas Scientific) to a size of 40 mesh. The extraction was performed using an ASE 350 Accelerated Solvent Extractor (Dionex, Sunnyvale, CA, USA). The two-step cyclic OS extraction method was performed with a preceding 2-hour hydrothermal extraction (water, 160°C, with a fixed volume of 40 ml at 110 bar). The lignin was extracted using 15 cycles, where one cycle had a duration of 5 minutes, and approximately 20% of the extract was displaced by a new solvent. The solvent composition of ethanol: water (70: 30 v/v) with 1.5 wt% sulfuric acid, at 160 °C, 110 bar, was used in Paper I, IV and V. In the trend series in Paper I, one cycle with a duration of 5 minutes was used for the two different solvent compositions, ethanol: water (70: 30 v/v) with 0.5 wt% or 1.5 wt% sulfuric acid, at 160 °C, 110 bar. In Paper II, the solvent composition and temperature were altered according to the design matrix of Box Behnken. For the one-step cyclic OS extraction method, Paper III, the wood sample was impregnated for 3 hours by the extraction solvent (ethanol: water (70:30 v/v with 1.5 wt% sulfuric acid) at ambient temperature. The lignin extraction was performed in 4, 9, or 15 cycles with a cycle duration of 5 minutes using the solvent composition of ethanol: water (70:30 v/v) with 1.5 wt% sulfuric acid, at 140 °C or 160 °C, 110 bar.

For the reference OS extraction method, the lignin extraction was performed with (Paper I and V) or without (Paper II) the preceding hydrothermal extraction described for the two-step cyclic OS extraction method. The lignin was extracted for 2 hours (Paper I, II, V) or 3 hours (Paper I) using the solvent composition of ethanol: water (70:30 v/v) with 1.5 wt% sulfuric acid, at 160 °C (Paper I, V) or 170 °C (Paper II), 110 bar. For all extractions (Paper I-V), the ethanol from the lignin-containing extract was evaporated by rotary evaporation under reduced pressure. The precipitated lignin was filtered and washed with water.

2.2 Characterization techniques

2.2.1 Nuclear Magnetic Resonance (NMR) spectroscopy

The Bruker NMR spectrometer Avance III HD 400 MHz instrument with a 5 mm Z-gradient BBFO broadband smart probe (Bruker Corporation, Billerica, MA, USA) and the Bruker 400 DMX instrument with a 5 mm Bruker BBI probe (Bruker Corporation, Billerica, MA, USA) were used for the NMR experiments.

HSQC NMR (^{13}C-^{1}H correlated) was performed for the extracted lignin by dissolving 80 mg of lignin in 600 µl deuterated dimethyl sulfoxide (DMSO). The spectra were acquired using the "hsqcetgpsi" pulse program. The quantitative ^{31}P NMR analysis was performed based on previously reported methods [60, 61]. Briefly, 30 mg lignin was phosphorylated by 2-chloro-4,4,5,5-tetramethyl-1,3,2-dioxaphospholane and dissolved in deuterated chloroform. The spectra were acquired using the "zgig30" pulse program. ^{13}C NMR analysis was performed by dissolving 80 mg of lignin in 600 µl deuterated DMSO together with 0.01 M chromium(III) acetylacetonate. The spectra were acquired using the "sd_zgig90" pulse program. All NMR data were collected and processed using MestReNova (v.9.0.0, Mestrelab Research). The interunit linkages were semi-quantified by HSQC NMR using the aromatic C_2 signal as an internal reference [62]. The quantification by ^{13}C NMR [63] was based on assuming six carbons and 0.12 vinylic carbons in the aromatic region, setting the integral to 6.12, and using this region as an internal standard [64]. The quantification by ^{31}P NMR was performed relative to an internal standard (*endo*-*N*-hydroxy-5-norbornene-2,3-dicarboximide).

2.2.2 Size Exclusion Chromatography (SEC)

SEC was performed using a DMSO system (Paper I) and a THF system (Paper II-V). Shortly, 9 mg lignin was dissolved in 2 ml of a 0.5 wt% lithium bromide in DMSO mixture for analysis using the DMSO system. The SEC system (SECurity 1260, Polymer Standards Service, Mainz, Germany) was equipped with refractive index (RI) detection. For the THF system, to increase the solubility of lignin in THF, the samples were acetylated prior to analysis, based on a previously reported method [65]. The SEC equipment setup comprised an autosampler (2707), HPLC pump (515), and photodiode detector (2998), (Waters Milford, MA, USA) with ultraviolet (UV) detection, operating at 254 nm. The calibration was performed using pullulan standards for the DMSO system and polystyrene standards for the THF system.

2.2.3 Carbohydrate analysis

Carbohydrate analysis and lignin content determination were performed according to protocols [66-68]. Briefly, the hydrolysis was performed on 200 mg of wood or extracted fibers (40 mesh), adding 3 ml of 72% sulfuric acid, followed by vacuum incubation for 80 minutes and heating in an autoclave for 60 minutes at 125 °C. The insoluble fraction, i.e., Klason lignin, was filtered, and the content was determined gravimetrically. The filtrate was used to determine the acid-soluble lignin content by UV-detection and for the carbohydrate analysis by a high-performance anion-exchange chromatography (HPAEC) equipped with pulsed amperometric detector (PAD) (Dionex, Sunnyvale, CA, USA) system using a previously reported method [69].

2.2.4 Matrix-assisted laser desorption/ionization-Time-of-flight-Mass spectrometry (MALDI-TOF MS)

Lignin samples were prepared for matrix-assisted laser desorption/ionization (MALDI)- time of flight (TOF) mass spectrometry (MS) analysis in a concentration of 0.05 mg/ml in DMSO, which was further mixed with the matrix (10 mg/ml 2,5-Dihydroxybenzoic acid (2,5-DHB) in TA30 (30:70 (v/v) acetonitrile: 0.1% trifluoroacetic acid in water) in a 10:1 ratio (v/v) matrix: lignin. 0.5 µl droplets were applied on the MALDI plate and analyzed using a Bruker ultrafleXtreme (Bruker Daltonik, Leipzig, Germany) instrument equipped with reflectron and Nd: YAG laser (355 nm).

3 Results and discussion

3.1 Protecting the lignin structure (Paper I)

3.1.1 Development of a physically protective extraction method

As previously discussed, lignin obtained by existing extraction processes suffers from a complex heterogeneous structure with poorly defined properties. Herein, the question was whether it was possible to extract lignin with preserved structure using a method based on the organosolv (OS) solvent system. Lignin with preserved native structure has the benefit of less structural complexity when compared to available technical lignins and can be a good starting point for valorization studies. A physical protection strategy to retrieve the lignin would yield a less modified lignin when compared to a classic OS batch lignin. To investigate possibilities for physically protecting lignin during extraction, a cyclic extraction strategy was adopted and was the main focus of Paper I. The emphasis was on the fundamental understanding of the concept, the methodology, and lignin properties. Combining the cyclic method for lignin extraction with a consolidated biorefinery conceptual view, a two-step extraction method/process was evaluated for obtaining the main polymers in spruce. The first step comprised a hot water extraction to extract the main part of the hemicellulose, using conditions already reported [70]. This was followed by the cyclic OS lignin extraction, Figure 5. To create physical protection to preserve the lignin structure, the method was designed so that only a part of the extract was needed to be exchanged with a new solvent during every cycle.

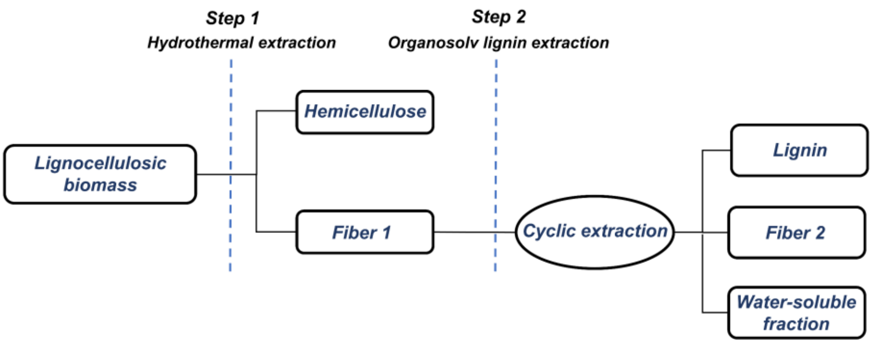

Figure 5. The two-step extraction method, where step 1 comprises the hydrothermal extraction to obtain hemicellulose, followed by step 2 where lignin is obtained by the organosolv lignin extraction.

As a measure of the degree of structural protection, native interunit linkages and functionalities were characterized and quantified by different NMR techniques. High-purity lignin was obtained with no or trace signals of carbohydrates detected by HSQC NMR. Signature signals for carbohydrates (free from overlapping lignin signals) appear in the anomeric region at 4-5/90-105 ppm (Paper I, SI Figure S3-S16 and S20). The mechanism behind the purity is likely due to the hydrolysis reactions that could occur within the lignin molecule, Figure 6 (II), or at lignin-carbohydrate bonds (LCC), Figure 6 (I). This creates lignin fragments with different molecular weights. Although the hydrolysis is not selective and affects the carbohydrates, the amount of carbohydrates in the recovered extracted lignin was low, as the sugars were retained in the water-soluble fraction.

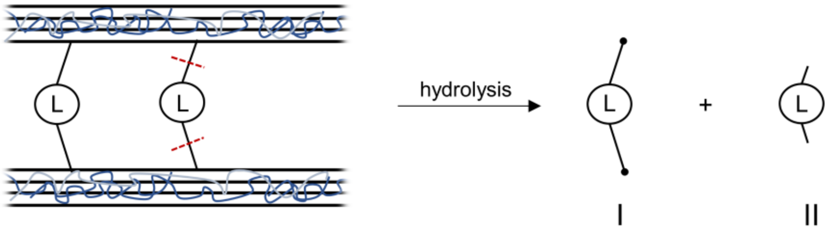

Figure 6. Illustration of the hydrolysis positions on the lignin molecules (L) under the extraction by the hydrolysis of LCC bonds (I) and hydrolysis within the lignin molecule (II). In (I), the dots on the end of the line illustrate the positions of a former LCC connection. In (II), hydrolysis occurred within the lignin chain. The horizontal rods illustrate the cellulose microfibrils separated by lignin and hemicellulose.

To investigate the impact of the physical protection concept through the cycles in the cyclic OS extraction, reference batch OS extraction was performed, where the same extraction conditions were used as for the cyclic OS extraction except for the cycles in step 2, Figure 5. The reference batch extraction was performed for 2 and 3 hours. The reference and cyclic OS lignin extraction were performed at 160 °C using the binary solvent composition of 70: 30 ethanol: water (v/v) and 1.5 wt% sulfuric acid at around 110 bar. The lignin yield was determined gravimetrically, the hydroxyl functionality by ^{31}P NMR, and the interunit linkages were semi-quantified by HSQC NMR. The molecular weight distribution and the dispersity (Đ) were estimated by SEC (DMSO system).

The cyclic OS extraction method was investigated using 5 min cycles in a total of 15 cycles with an effective extraction time of approximately 1 hour and 15 minutes. Two different acid concentrations were explored, i.e., 0.5 wt% and 1.5 wt%. To increase the understanding of the kinetic of the lignin extraction, determined by the yield and how the chemical properties were changed between the cycles, extract from every cycle was collected and analyzed separately. It was shown that most of the soluble lignin was extracted in the first four cycles. Practically, from the tenth to the eleventh cycle, the sample amount was not enough to be characterized by the analytical methods. After the individual investigation of the lignin properties in each cycle, a final method was developed to collect the cycles together in an integrated method.

The native- and formed lignin structures are shown in Figure 7. The β-O-4′ interunit linkages were particularly interesting since they are the most common interunit linkage in lignin [6] and contain labile ether bonds that are more easily hydrolyzed than carbon-carbon bonds under acidic conditions. For this reason, the β-O-4′ content was used as an indicator for the mildness of the extraction.

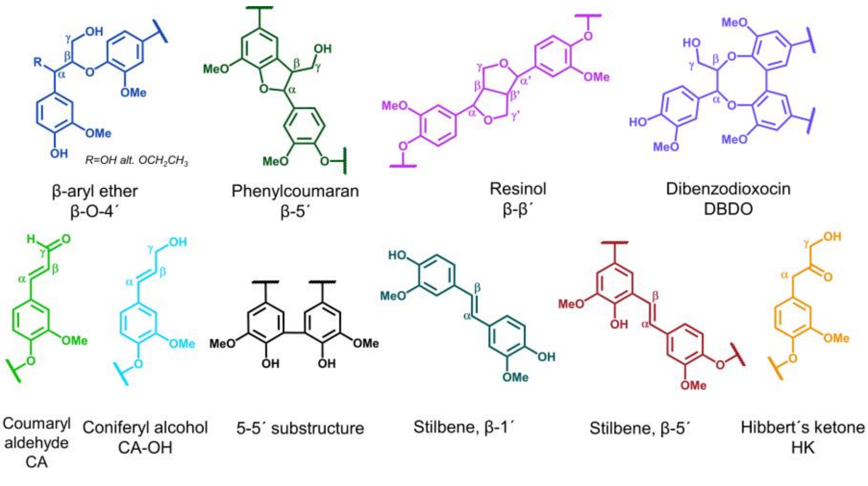

Figure 7. Interunit linkages and substructures of lignin identified by HSQC NMR analysis.

Distinct signals assigned to ArC$_2$-H and ArC$_6$-H correlations in 5-5′ condensed structures [42] at 6.7/112.5 ppm and 6.6/120.5 ppm (Figure 8) were observed for the batch extracted sample. These were shifted from the non-condensed structures at 6.92/100.5 ppm and 6.8/118.5 ppm. This signature of 5-5′ condensed structures was less significant for the cyclic extracted OS lignin, Figure 8.

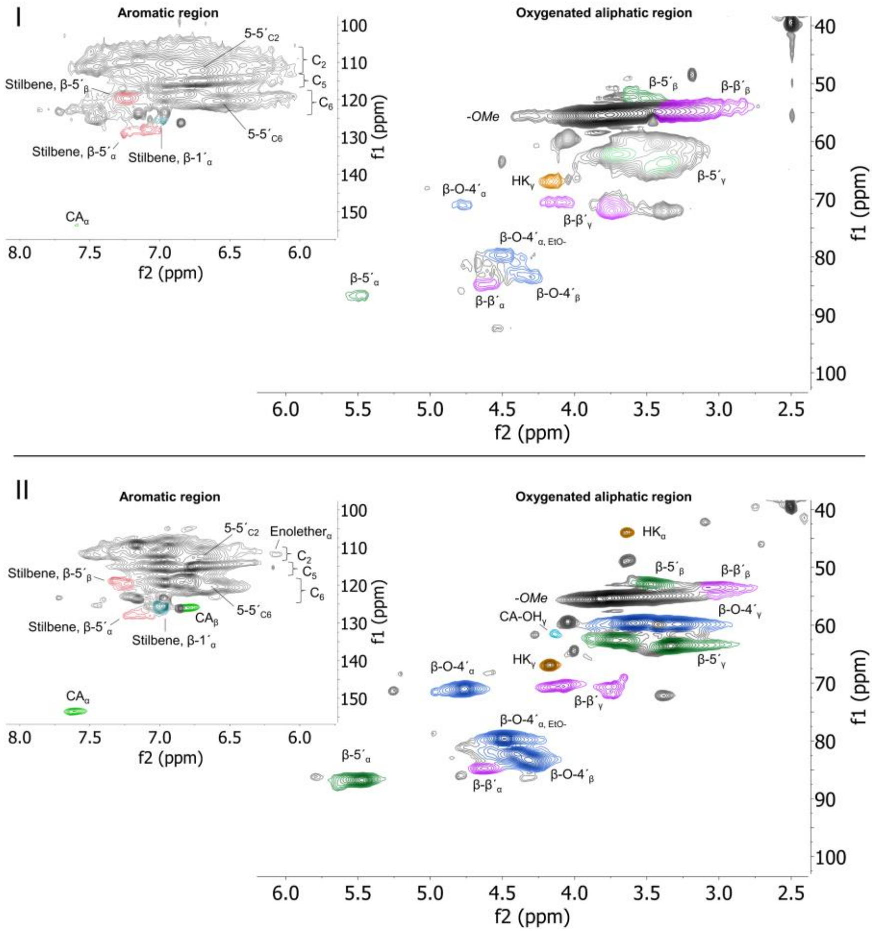

Figure 8. HSQC NMR spectra of the 2-hour OS reference extracted lignin (I) and the integrated cyclic OS extracted lignin (II), obtained at 160 °C using 1.5 wt% sulfuric acid by the two-step extraction method.

The lignin obtained from the reference extractions showed characteristics typically identified for OS lignin, Figure 3 and Table 1, such as low content of β-O-4′ interunit linkages in a range of 7-4% with both etherified and hydroxylated C_α position. The degree of etherification of C_α was in the range of 60-70% for the cyclic extracted lignins and over 70% for the reference lignins.

Table 1. Semi-quantification of interunit linkages by HSQC NMR for the reference OS lignin and cyclic OS lignin (by the integrated method). The β-O-4′$_α$ includes both hydroxylated and etherified C$_α$ positions.

Lignin	β-O-4′$_α$	β-5′$_α$	β-β′$_α$	Stilbene, β-1′$_α$ *per 100 Ar*	Stilbene, β-5′$_β$	CA$_α$	HK$_γ$	Yield [mass%]
2h	7	6	1.5	0.84	6.1	0.41	1	56
3h	4	5	1.1	n.d.[1]	4.3	n.d.	0.26	69
Cyclic	30	12	2.4	4.4	3.9	2.0	1.3	53

[1]n.d.=not detected.

A major part of the lignin was extracted in the first four cycles with a steep slope that declined from cycle number five to ten. A similar trend was shown for the yield, whether 1.5 wt% or 0.5 wt% sulfuric acid was used in the solvent compositions, Figure 9.

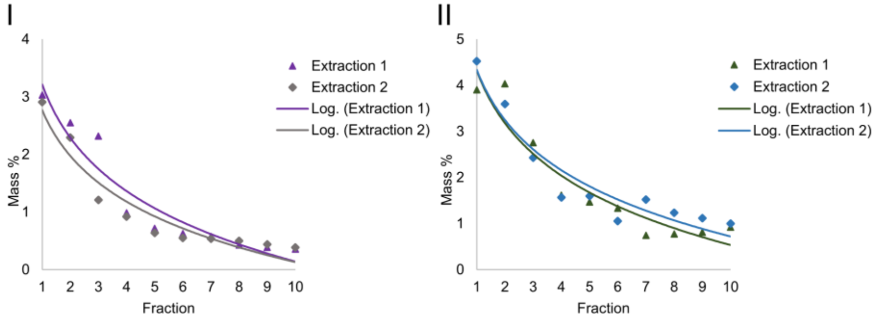

Figure 9. The trend of the yield for lignin extracted using 0.5 wt% sulfuric acid (I) and 1.5 wt% sulfuric acid (II). The average mass % of extracted lignin based on the starting mass of fiber was 11.2% for (I) and 18.1% for (II).

The total lignin yield (53.3%) for the shorter integrated cyclic OS extraction method (approximately 1 hour and 15 minutes) was in the same range as the lignin yield from the OS reference 2 hours' extraction (56.3%). This might be explained by the effects of a less saturated solvent attributed to the partial displacement of the extract by the new solvent in every cycle. The yield of hemicellulose in the hydrothermal extraction was 16 ± 1.4 mass %, number of replicates, n=3.

The aliphatic hydroxyl content was significantly higher for the cyclic extracted lignin (2.8 mmol/g) than for the OS reference lignin (1.6 mmol/g). This indicates a high preservation of the native aliphatic configuration of hydroxy groups on the benzylic side-chain on the lignin molecule. Studying the individual cycles, the trend of aliphatic hydroxyl functionalities was slightly decreased from cycles 1 to 9; however, they were still at relatively high levels Figure 10 (I). The decrease was likely due to a combination of increasing etherification of lignin and the occurrence of side-reactions. The trend of non-condensed phenolics (i.e., guaiacyl hydroxyls) shows a slight decrease from the 1 to 3 cycles, followed by no distinctive changes. This aligns with the general stable trend of β-O-4′ interunit linkages from the fifth cycle, Figure 10 (II).

The trend of β-O-4′ and β-5′ interunit linkages was investigated for cycles 1-9, Figure 10 (II). Interestingly, the content of β-O-4′ and β-5′ interunit linkages was at a lower level for the first cycle but higher in the second cycle, followed by a slight decline and then stabilized from the fifth cycle. The lower content of β-O-4′ and β-5′ interunit linkages in the first cycle might originate from hydrolysis reactions during the hydrothermal extraction in the first step. At such conditions, autohydrolysis, catalyzed by acetic acid originating from the acetyl-groups released from hemicellulose, has been reported [71]. It was hypothesized that the structures with lower β-O-4′ contents in the first cycle were formed in the first hydrothermal step and were more easily extracted in the subsequent step. These structures also had a higher content of non-condensed phenolics, Figure 10 (I). From the investigation of the molecular weight distribution by SEC, the distribution curve for lignin obtained from the two first cycles had one symmetric signal and lower molecular weight than lignin obtained from the third to the tenth cycle, Figure 10 (III).

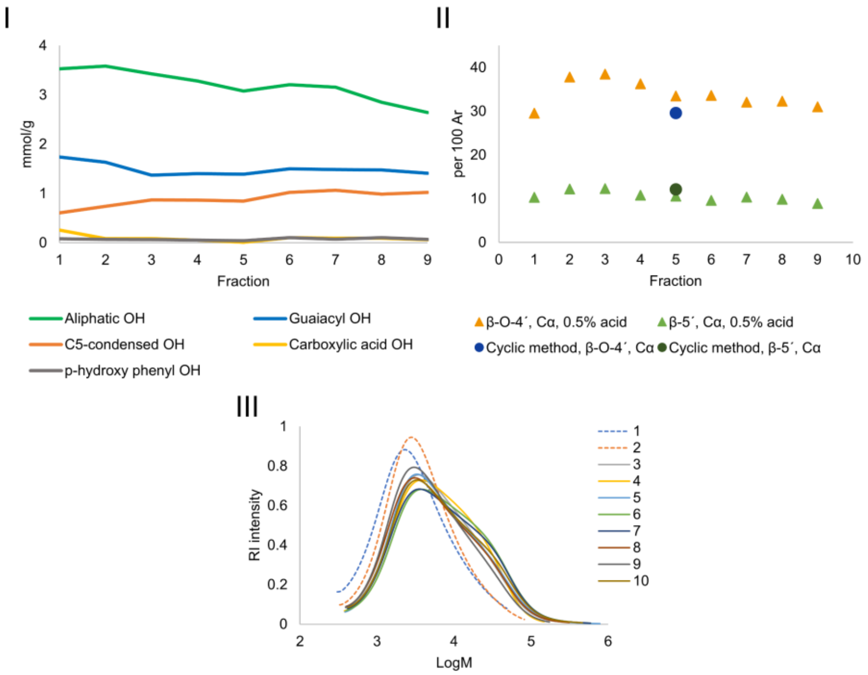

Figure 10. The trend of the hydroxyl content (I), β-O-4′ and β-5′ content (II) and molecular weight distribution (III).

A similar trend of preserved β-O-4′ interunit linkages was shown for lignin extracted using both 0.5 wt% and 1.5 wt%, where the β-O-4′ content was in the range of 30-38%, Figure 10 (II). This value is similar to milled wood lignin (MWL) obtained from softwood, which is reported at about 35% [72].

Another interesting feature of the extracted lignin was the color. Using the cyclic OS extraction method, the retrieved lignin appears to have a brighter light-beige color Figure 11 (I) compared to the lignin obtained in the batch extraction (II and III). Worth to note is that the first cycle extract was darker than the subsequent cycles, which may support the earlier speculation on this being a modified lignin or lignin contaminated with degradations products from carbohydrates formed during the preceding hydrothermal extraction.

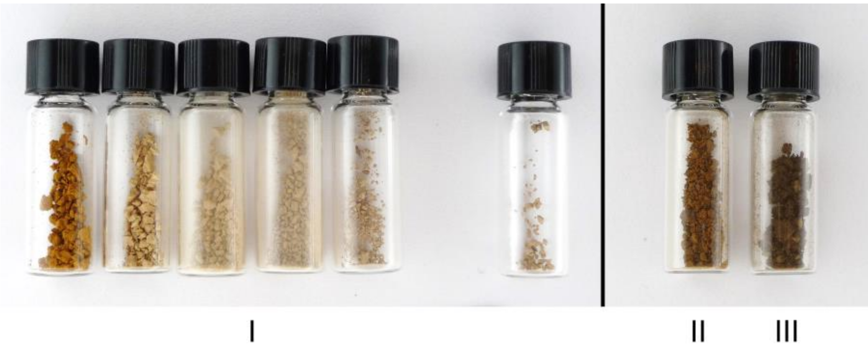

Figure 11. Lignin fractions extracted with 0.5 wt% sulfuric acid, in the order of fractions 1-5 and fraction 10 (I), and the OS reference lignin, which was obtained in a 2-hour (II) and 3-hour (III) batch extraction.

To decrease the dispersity (Đ) of the lignin obtained using the integrated cyclic OS extraction method (Đ of 4.5), fractionation with ethanol was performed. The ethanol soluble and insoluble fractions were obtained in a yield of approximately 48% and 52%, respectively, with a Đ of 2.2 for the ethanol soluble fraction and a Đ of 3.7 for the insoluble ethanol fraction. The degree of polymerization (DP_n) was 7 for the unfractionated lignin, 4 for the ethanol soluble, and 13 for the insoluble fraction. It is worth noting that these values are always relative to the solvent system used in the analysis and that lignin analysis by SEC methods still suffers from several problems, including association effects and lack of representative standards, to mention a few. Therefore, these values should only be interpreted in a comparative manner between the samples. To determine DP_n, 180 Da was used as an estimated monomer reference for lignin, corresponding to coniferyl alcohol, Figure 1. The ethanol soluble and insoluble lignin fractions had a similar content of β-O-4′ interunit linkages at around 30%, characterized by HSQC NMR.

In summary, a lignin with preserved structure could be obtained using the cyclic OS extraction method, manifested by the preserved β-O-4′ interunit linkages. The method was based on a physical protection concept, where only a part of the solvent was exchanged in a plurality of cycles to retrieve lignin with preserved structural integrity. There was no need for chemical additives to protect the lignin structure.

The less saturated extract environment decreased the probability of intermolecular reactions such as condensations of the dissolved lignin. The opposite scenario was observed for batch extraction. Interestingly, the main part that could be extracted using the investigated extraction conditions were extracted in the beginning. Another advantage of the cyclic OS extraction method was that a similar yield to batch extraction could be obtained without compromising lignin quality (defined by structural preservation). The cyclic OS extraction might also offer opportunities to study lignin from different locations in the cell wall.

3.2 Tailoring of chemical properties (Paper II)

Understanding how the extraction parameters affect the properties of lignin is important for fundamental insights into reactivity, for lignin valorization, and for targeting application needs.

Thus, a chemometric study and design of experiment (DoE) approach was used to further investigate the tailoring potential of the cyclic OS extraction concept. Accordingly, the dependence of the factors on selected properties was evaluated using DoE and multivariate analysis. By DoE, the experimental data is used in mathematical models according to the selected design model. Most often, the factors have more than only a linear dependence on the response, and without using a model that includes not only linear but additionally quadratic and interaction relations, there is a risk that the evaluation of the relation between the factors and property will be poor [73]. For method development and optimization, DoE is time and cost-efficient compared to the “one-variable at a time” approach, and there is a risk that the optimum cannot be found using the “one-variable at a time” approach. The selected model depends on the research purpose, where a linear screening model can be used to find the significant factors to reduce the number of experiments, such as the Plackett-Burman design, followed by a quadratic model that includes more relations [74, 75].

One quadratic design is the Box Behnken design, which does not include corner points [76]. Using three factors at three levels, including three center points, the design matrix consists of 15 experiments. In these experiments, the factors were changed according to defined levels within the design domain. From the significant models for the different responses, the models can be used to predict responses within the experimental domain and to find optimal conditions for a certain desired criterion [73, 74]. The DoE approach has been used in the lignin field to find optimal conditions for ionization in mass spectrometry analysis of lignin [77] and in the synthesis of lignin-containing materials [78].

3.2.1 Chemometric study of the protective extraction method

Is it possible to tailor the lignin properties using the developed cyclic physical protecting extraction concept? The hypothesis was by using chemometrics, such as multivariate analysis and DoE, the impact of the extraction parameters on the lignin properties could be evaluated. The selected properties and extraction conditions are illustrated in Figure 12.

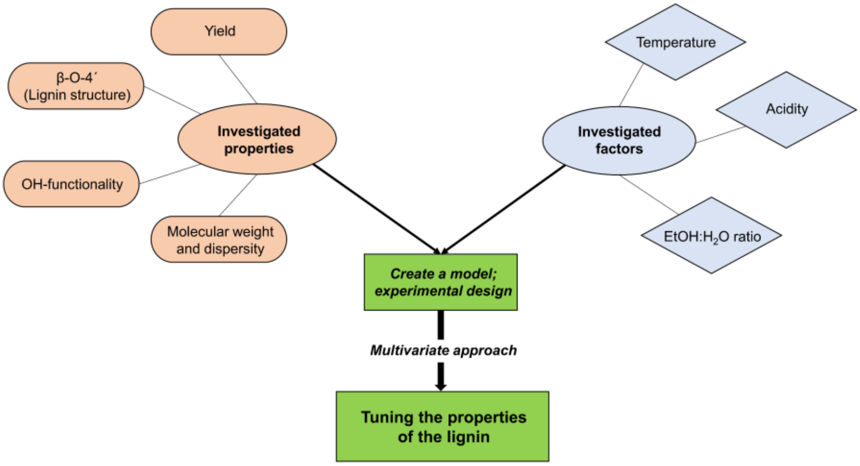

Figure 12. Illustration of the set-up of the chemometric study, with selected factors and lignin properties. Figure adapted from Paper II [79] with permission from the Royal Society of Chemistry.

The same two-step extraction method was used for all the design extractions where lignin was obtained from spruce wood. The second-order Box Behnken design was selected, which includes linear, interaction and quadratic terms. The question was how the structural property of lignin was affected by the temperature, sulfuric acid concentration and ethanol: water ratio. The factors that were quantitatively investigated, including the ranges, are shown in Table 2.

Table 2. The quantitatively investigated factors with the assigned variable range.

Factor	Variable range -1	0	1	Unit
Temperature	110	140	170	°C
Acid	0.5	1.5	2.5	wt%
Ethanol: water	60:40	70:30	80:20	v/v

The experimental data were fitted with multiple linear regression (MLR). Significant models were obtained for all the investigated lignin properties, Figure 12, defined by the variance explained by the model, predictability of variation from cross-validation, model validity and reproducibility. The characterization methods were as described for the previous study, i.e., ^{31}P NMR for hydroxyl functionalities, HSQC NMR specifically for β-O-4′ content, SEC (THF system) for molecular weight, and the lignin yield was determined gravimetrically.

3.2.2 Correlation between extraction parameters and lignin properties

The effect of the different factors on the lignin properties was evaluated within the experimental domain by the magnitude and whether they affected the lignin property positively or negatively. The correlation between the lignin properties and factors is shown in the response surface plots in Figure 13. The ethanol concentration was fixed on the middle level of the variable range since the temperature and acid concentration were shown by the model to have the highest overall significance for the investigated lignin properties.

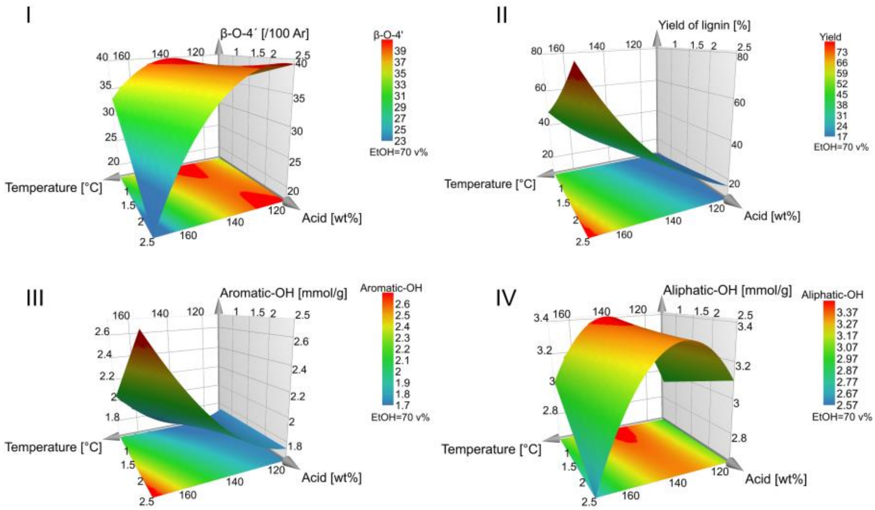

Figure 13. The factor dependence, by the temperature and acid concentration on the β-O-4′ content (I), the yield (II), the aromatic hydroxyl content (III), and the aliphatic hydroxyl content (IV), illustrated by the response surface plots.

The β-O-4′ interunit linkages and aliphatic hydroxyl content showed a similar trend with a complex relation, where the content was negatively affected by the quadratic effects of the temperature and ethanol: water ratio together with an interaction effect of temperature x acid concentration. Similar content of β-O-4′ interunit linkages could be obtained at lower temperatures with higher acid concentration as for slightly higher temperature and lower acid concentration, a trend not shown for the aliphatic hydroxyl content. Correlating these results, it can be speculated that at low temperatures and higher acid concentrations, reaction on the aliphatic side-chain was more prone to occur than the cleavage of β-O-4′ interunit linkages.

Only linear terms were significant for the yield, Figure 13 (II), including the temperature and acid concentration showing a positive influence. The most significant positive relative effect on the yield was by the temperature, which had the largest negative effect on the content of β-O-4′ interunit linkages. This implies that obtaining a high content of β-O-4′ interunit linkages simultaneously as high yield was not applicable within the experimental domain, wherein a compromise might be necessary. This relation can be visualized in Figure 13 (I and II), where the lowest content of β-O-4′ interunit linkages (I) was where the highest yield could be obtained (II). The negative influence on the β-O-4′ interunit linkage content and aliphatic hydroxyl content from the quadratic ethanol: water ratio was further investigated where the optimal ratio of the whole range of acid concentration and temperature was at 70:30 ethanol: water (v/v) ratio. As illustrated in (I) and (IV), the highest content of β-O-4′ and aliphatic hydroxyl content was obtained at around 140 °C using the solvent composition of 70:30 ethanol: water (v/v) and 1.5 wt% sulfuric acid.

The aromatic hydroxyl content Figure 13 (III) had a positive influence from the interaction effect of temperature x acid concentration and the quadratic effect of the temperature together with the linear terms of temperature and acid concentration. The highest content of aromatic hydroxyls was obtained at the highest temperature and acid concentration within the experimental domain, i.e., at 170 °C and 2.5 wt% sulfuric acid, which is consistent with the extensive depolymerization by the cleavage of β-O-4′ linkages yielding free phenolic moieties. Nevertheless, by using the two-step cyclic OS extraction method, the content of β-O-4′ interunit linkages at the most severe conditions within the experimental domain was still in the range of 20 per 100 Ar, in contrast to the OS reference lignin produced in a single 2-hour batch extraction at same conditions, with a β-O-4′ content of 7 per 100 Ar. Within the investigated range of the factors, the ethanol: water ratio showed no significance by the model on either the aromatic hydroxyl content or the yield of extracted lignin.

The number average molecular weight (M_n) and Đ were analyzed by SEC. The significant factors for M_n showed a negative effect for the quadratic term of temperature and a positive effect for the linear terms of the temperature and acid concentration. The Đ showed a positive influence from the interaction effect of temperature x ethanol: water ratio, the quadratic effect of the temperature and the linear terms of temperature and ethanol: water ratio. Both M_n and Đ were highest for lignin obtained at higher temperatures and acid concentrations. This effect might result from a more pronounced repolymerization causing both an increase of the molecular weight, consistent with OS extraction reactions at severe conditions, and an increase of Đ. An alternate explanation is that larger pores are formed in the fibrils to enable the extraction of larger macromolecules.

The hemicellulose and water-soluble fraction, Figure 5, were analyzed by HSQC NMR to elucidate the chemical properties. The properties of the hemicellulose fraction were already investigated in Paper I by HSQC NMR with typically expected characteristics from native hemicelluloses, such as retained *O*- acetylation groups. The water-soluble fraction was defined as the filtrate obtained after removing ethanol and subsequent filtration of the precipitated lignin. HSQC NMR analysis showed predominantly products resulting from the acid-catalyzed depolymerization of the polysaccharides, i.e., mono-sugars and dimers. The fiber 2 fraction, Figure 5, was investigated by powder X-ray diffraction to investigate the crystallinity, where the fiber residues from the two-step process appear to retain the crystallinity seen from the pattern (Paper II). The fiber 2 fraction had different properties dependent on the OS lignin extraction conditions, which varied at the different design entries. It mainly constituted of cellulose (65-80%), but dependent on the extraction conditions, it contained lignin as well (12-30%) and trace amounts of hemicellulose.

In summary, the results from the chemometric study gave an insight into the relation between selected extraction parameters and lignin properties. Furthermore, insights into the tunability of lignin properties were obtained. This is of relevance for target applications. Lignin with high content of β-O-4′ interunit linkages might be suitable for depolymerization to platform monomers, using for instance reductive catalytic fractionation or hydrogenolysis [51, 80-82]. On the other hand, lignin with low Đ and DP_n might be suitable as a precursor for the synthesis of thermosets, where the aromatic and aliphatic hydroxyl functionalities might serve as chemical handles for further modifications of relevance for material synthesis [83, 84]. The content of aromatic or aliphatic hydroxyls can be tuned based on the correlation of properties and extraction conditions shown by the DoE study. The three center points, i.e., replicates, show significant reproducibility for all investigated properties, Figure 12, and illustrate the robustness of the two-step cyclic OS extraction method.

3.3 A flexible biorefinery concept; One-step process (Paper III)

As mentioned in *section 3.2.2*, even though the focus of the study was primarily on the lignin fraction, the other streams are also of importance. This reflects the principle of a consolidated biorefinery, where several parts should be considered for their value. To be able to do a proper evaluation of the potential value, knowledge about the properties of the components in the different streams is fundamental. This knowledge will assist in further understanding the potential for different routes, and this defines the flexibility investigated within this study. For an efficient process, using as few steps as possible to minimize the loss of material and energy is desirable [56]. Furthermore, reducing the usage of associated solvents and chemicals is advantageous. The efficiency of reducing the steps from a two- to a one-step process, as well as reducing the number of cycles and the temperature, was investigated.

3.3.1 A one-step extraction method

Is it possible to refine the steps of the cyclic OS extraction method with retained lignin quality and overall yield and simultaneously tailor the fiber properties?

The one-step cyclic OS extraction method, Figure 14, was evaluated in terms of versatility and robustness by studying two types of wood species; spruce as a representative for SW and birch as a representative for HW. The difference between the one-step and two-step processes, described in *section 3.1.1*, was the exclusion of the hydrothermal hemicellulose extraction step (2 hours at 160 °C).

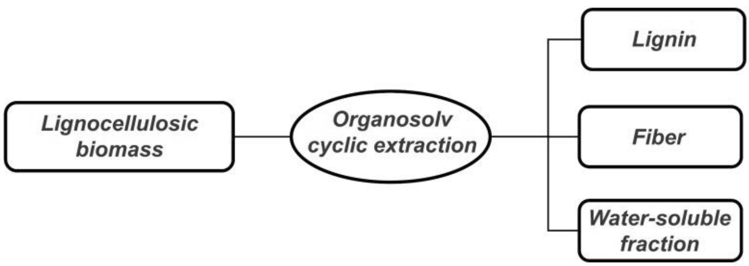

Figure 14. Illustration of the one-step cyclic OS method with the different streams by the lignin, fiber, and water-soluble fraction.

As previously, the preservation of lignin structure was evaluated by the content of β-O-4′ linkages, *section 3.1.1*. Based on the results from the chemometric study presented in *section 3.2.1*, the one-step extraction method was investigated using the optimal temperature and solvent composition for the highest content of β-O-4′, i.e., at 140 °C using the binary solvent system of 70:30 ethanol: water (v/v) together with 1.5 wt% sulfuric acid.

Based on the yield of lignin extracted in each cycle, *section 3.1.1*, where the main part of the lignin was extracted in the first cycles, the selected number of cycles was 4 and 9 in the evaluation of the one-step extraction method. Using this approach, an investigation was made to see if it was possible to obtain a fiber residue with maintained carbohydrate composition. Apart from the stated optimal conditions, other conditions were also used to evaluate differences between the one-step and two-step approaches in terms of yields, compositions, and lignin structure outcomes. This was 15 cycles extraction at 160 °C. An additional investigation was made to evaluate the effects of sequential lignin extraction. Accordingly, a gradient-type extraction was performed with 4 cycles at 140 °C followed by additional 4 cycles at 160 °C. The birch wood, used to investigate the universality of the method, was extracted using 9 cycles at 140 °C.

3.3.2 Preserving the properties of the lignin and fiber

Based on HSQC NMR analysis, all lignin within the study showed high purity with a carbohydrate content estimated to <1%, visualized by the signal from the C_1-H correlation in mannan at 4.6/101.4 ppm. There were no clear signs of extensive 5-5′ condensations in the aromatic region, causing the shifting from the non-condensed structures at 6.9/100.5 ppm and 6.8/118.5 to the condensed at 6.7/112.5 ppm and 6.6/120.5 ppm for the ArC_2-H and ArC_6-H correlations, Figure 15. Native structures, such as dibenzodioxocin (DBDO), Figure 15, were preserved, indicating a mild extraction path to obtain the lignin from the wood.

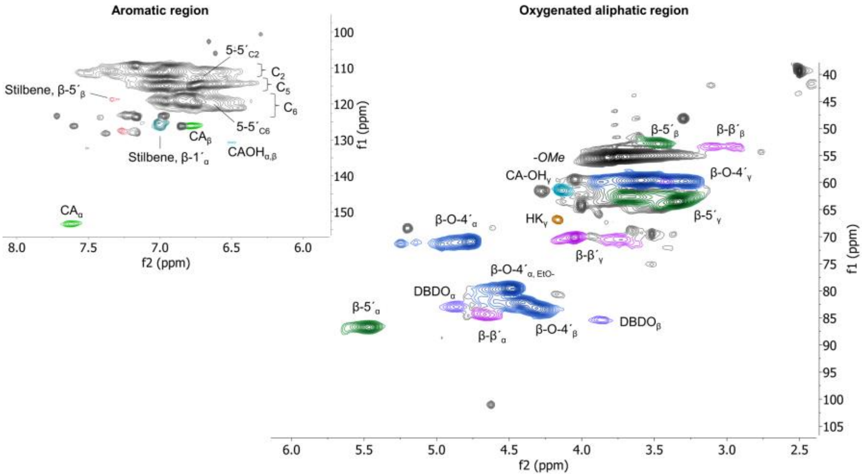

Figure 15. HSQC NMR spectra of lignin from spruce obtained by a 9-cycle extraction at 140 °C. The spectra are assigned according to the structures in Figure 7.

The semi-quantification of interunit linkages, Figure 7, is listed in Table 3. The content of β-O-4′ linkages for the extracted spruce lignins was 53% and 54% (%; per 100 Ar) at extraction conditions of 140 °C using 4 and 9 cycles, respectively. The validity of the semi-quantification of β-O-4′ interunit linkages by HSQC was verified by ^{13}C NMR. Here, the signal at 61.4-58.3 ppm, corresponding to the C_γ position in the β-O-4′ structure [85] (Figure 7) was used in the quantitation, yielding values in a similar range of 53% and 52%. These values are close to the theoretically reported values for β-O-4′ content in softwood (60%) [6], and higher than those reported for MWL [7].

Comparing the content of β-O-4′ interunit linkages for the lignin obtained at 140 °C with the lignin obtained at 160 °C, there was a decrease to around 42% for the 4 cycles. As seen from the chemometric study discussed in *section 3.2.2*, the temperature negatively influences the β-O-4′ interunit linkage content. This was due to the acidolysis of the β-O-4′ ether bonds at higher temperatures [34]. However, even with the negative effect of temperature, the cyclic method still serves to protect the structure better than batch extraction, where the content of β-O-4′ interunit linkages is reported below 10% [36, 86].

Table 3. The semi-quantification of interunit linkages for spruce lignin by HSQC NMR. The fractions are labeled as follows; 4 cycles at 140 °C (1), 4 cycles at 160 °C immediately after a 4-cycle extraction at 140 °C (2), 9 cycles at 140 °C (3) and 15 cycles at 160 °C (4).

Lignin	**β-O-4′$_{\alpha}$**	**DBDO$_{\beta}$**	**β-5′$_{\alpha}$**	**β-β′$_{\alpha}$**	**Stilbene, β-1′$_{\alpha}$**	**Stilbene, β-5′$_{\beta}$**	**CA$_{\alpha}$**	**HK$_{\gamma}$**
				per 100 Ar				
1	53	1.6	13	2.2	6.3	1.9	2.7	0.75
2	42	0.5	12	2.1	3.4	3.3	2.6	1.6
3	54	2.3	14	2.2	4.0	1.1	2.7	0.75
4	31	1.6	10	2.1	4.8	1.4	1.8	1.3

As discussed in *section 3.3.1*, the versatility of the one-step cyclic method for different raw materials was investigated by applying the same concept developed for spruce wood to the HW specie birch. The HSQC NMR spectrum of birch lignin obtained using 9 cycles at 140°C is illustrated in Figure 16, with a β-O-4′ content of 67%. The universality of the physical protection through the cycles was hence verified for different wood species.

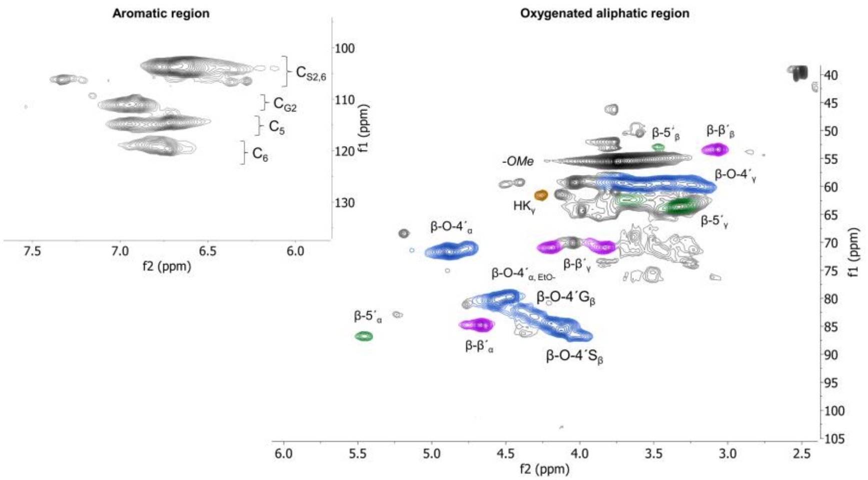

Figure 16. The HSQC NMR spectra of birch lignin by the 9-cycle extraction at 140 °C.

The M_n, Đ, and DP_n values were investigated for spruce and birch lignin by SEC (THF system), Table 4. Similarly, as presented in *section 3.1.1*, DP_n was determined using 180 Da as a representative molecular weight for a model lignin monomer. The birch and spruce lignin obtained using similar extraction conditions had a similar M_n. By increasing the extraction temperature, the M_n increased, which was also seen in the chemometric study, *section 3.2.2*, which might, in this case, be explained by the extraction of lignin fragments of higher molecular weight. This assumption was based on the fact that no substantial signs of condensation products by the NMR analysis at this extraction condition were seen. The assumption was further manifested in the lower Đ values for lignin extracted at lower temperatures. Higher Đ values are consistent with the occurrence of both depolymerization and repolymerization reactions simultaneously at higher temperatures. The lignin obtained at 140 °C, using 9 cycles, was further refined by ethanol fractionation to obtain an ethanol-soluble fraction (~60%) and an insoluble fraction (~40%). The Đ was improved and similar for both fractions, Table 4.

Table 4. The M_n, Đ and DP_n of the spruce and birch lignin obtained at different conditions using the one-step extraction method. The cycle is abbreviated by the C notation.

Lignin	M_n [g/mol]	Đ	DP_n
Spruce, 4C, 140 °C	2200 ± 30[2]	4.6 ± 0.04	12
Spruce, 4C, 160 °C[1]	3400 ± 20	4.7 ± 0.03	19
Spruce, 9C, 140 °C	2400 ± 20	6.0 ± 0.03	13
Spruce, 4C, 140 °C, EtOH soluble	1300 ± 30	2.3 ± 0.03	7
Spruce, 4C, 140 °C, EtOH insoluble	6600 ± 550	2.2 ± 0.09	36
Birch, 9C, 140 °C	2500 ± 30	4.1 ± 0.03	13

[1]The lignin was obtained by 4 + 4 cycles at 140 °C + 160 °C. [2]Number of replicates, n=2.

To obtain a more accurate estimation of the content of interunit linkages in the lignin oligomers, the HSQC NMR data was corrected for the molecular weight based on DP_n estimations from the SEC analysis. The correction was made only for interunit linkages, excluding end groups such as CA and HK. The equation for calculating the theoretical % of interunit linkages is shown in Eq. 1, where the M_n value was obtained from SEC, and DP_n value was calculated by using 180 Da as a monomeric reference for lignin.

$$Theoretical\ \%\ of\ interunit\ linkages = \frac{\left(\frac{M_n}{180} - 1\right)}{\frac{M_n}{180}} * 100 \qquad (Eq. 1)$$

The results from the correction show, for lignin obtained at 140 °C, that more than 95% of the lignin structure was assigned. Similarly, more than 85% of the structure was assigned for the lignin obtained at 160 °C. For comparison, the content of interunit linkages and substructures from the two-step process described in *section 3.1.1,* together with benchmarks such as kraft lignin (LignoBoost), is illustrated in Figure 17. Determining the content of 5-5′ interunit linkages is problematic due to overlapping signals. The signal at 132-133 ppm in ^{13}C NMR spectra of lignin has been assigned to the C_5 in 5-5′ units [85]; that region, however, suffers from overlapping signals. Another strategy is integrating the 5-5′$_{C2}$ signal in the HSQC NMR spectra, Figure 15, which, however, also suffers from overlap. Nevertheless, this signal was applied for the semi-quantification, with the awareness that the values could be overestimated.

Using similar quantitation principle for birch as for spruce, 85% of the birch lignin structure was assigned, Figure 17. The superior analytical quality of the cyclic OS lignin over the kraft lignin was demonstrated. Less than 50% of the kraft lignin structure could be assigned. This is consistent with the literature [42, 43]. Comparisons of the one-step and two-step extraction for spruce at similar extraction conditions showed that the β-O-4′ content was significantly higher for the one-step process (57% versus 40%). This is likely due to the cleavage of some β-O-4′ bonds during the hydrothermal extraction in the case of the two-step extraction.

Comparing the lignin structures between spruce and birch, Figure 17, the β-O-4′ contents were in close proximity to those reported for native lignin [6]. This demonstrates, as previously stated, the mildness of the method due to the physical protection and that the one-step process protects the lignin to a higher degree than the two-step process.

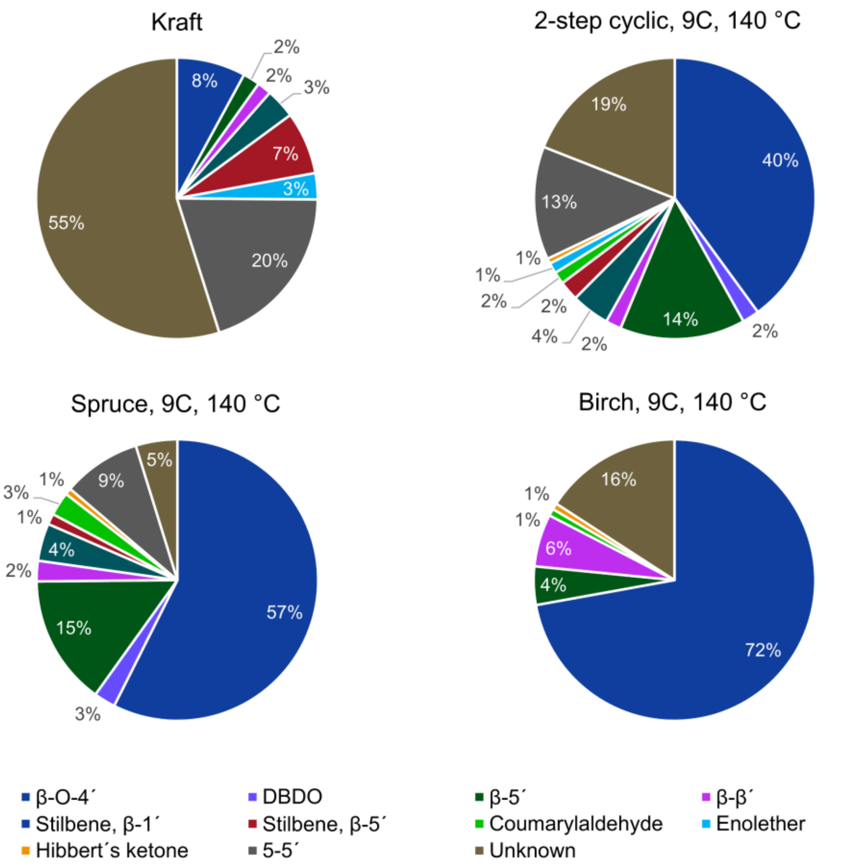

Figure 17. Theoretical % of interunit linkages. The number of cycles is abbreviated by the C notation. The linkages for kraft lignin from spruce, derived by the LignoBoost process, were semi-quantified based on HSQC NMR results from Paper II. The lignin retrieved from the two-step cyclic OS extraction is presented in Paper I, *section 3.1.1*. The “Spruce, 9C 140 °C” and “Birch, 9C, 140 °C" were retrieved by the one-step cyclic OS extraction method.

The effects of the monolignol composition on the lignin structure were also visible from the analysis, Figure 17. For instance, the lack of detection of β-5′ stilbene structures in birch lignin can be explained by the dominance of S units over G units in birch lignin. For similar reasons, higher content of β-O-4′ and β-β′ interunit linkages were observed in birch.

The hydroxyl functionalities of the spruce and birch lignin were studied by ^{31}P NMR. Overall, the lignin obtained by the one-step cyclic OS extraction method showed higher retention of the aliphatic hydroxyl functionalities explained by physical protection through the cycles. The increase of C_5 substituted phenolic hydroxyls at higher temperatures could be explained by the cleavage of β-O-4′ interunit in 5-5′ etherified sub-units, which in turn increases the content of phenolic moieties, identified by ^{31}P NMR. This is consistent with the enhanced cleavage of β-O-4′ bonds at higher temperatures [34]. In Figure 18, the hydroxyl functionality of the lignin obtained from spruce at 140 °C and 160 °C using 4 and 9 cycles, together with a benchmark Alcell-based extracted lignin, obtained using the same solvent system but in a 2-hour batch extraction at 160 °C, are reported. Unfortunately, sinapyl hydroxyl groups overlap with the region for C5-substituted hydroxyl and aliphatic hydroxyl in the ^{31}P NMR spectra. This complicates detailed comparisons between birch and spruce lignin in terms of different hydroxyl functionalities. However, the total hydroxyl content could be compared. Accordingly, for the lignin obtained at 140 °C using 9 cycles, the total content of hydroxyl functionalities was found to be in a similar region: 5.2 (birch) to 5.4 (spruce) mmol/g lignin.

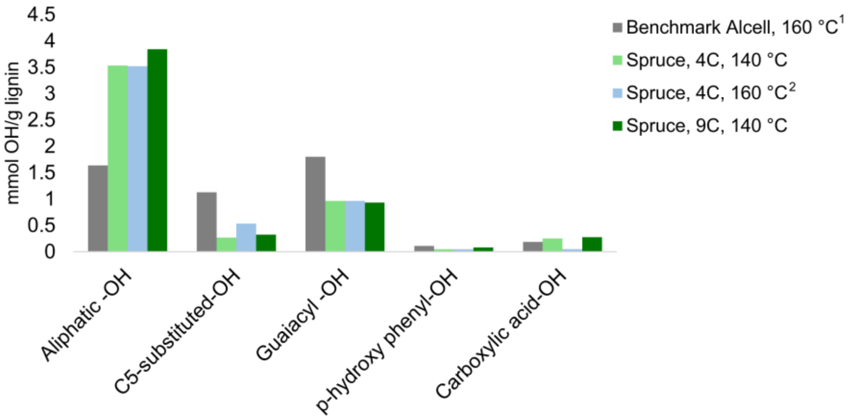

Figure 18. The hydroxyl functionalities of the spruce lignin, derived at different conditions, using the one-step extraction method analyzed by ^{31}P NMR, together with a benchmark Alcell-based extracted lignin. The number of cycles is abbreviated by the C notation. [1]Spruce lignin derived from Alcell-based extraction, in a 2-hour batch at 160 °C, from Paper I, *section 3.1.1*. [2]Lignin obtained by 4 + 4 cycles at 140 °C + 160 °C.

The color of the lignin derived from the one-step process was contrasted with that of sawdust, Figure 19. A similar color was obtained for lignin extracted at 140 °C and the stepwise extraction of 140 °C + 160 °C. The similarities in the color of the lignin product and raw material may also reflect the mild and protective nature of the process. Using the one-step method, lignin with bright color could already be obtained from the first cycle, unlike the lignin retrieved in the first cycle from the two-step method with the preceding hydrothermal extraction.

Figure 19. Sawdust and extracted lignin beside each other illustrate the color of the extracted lignin using the one-step extraction method. The color is representative of lignin obtained using 4 and 9 cycles at 140 °C and 4 cycles (at 140 °C) followed by 4 cycles (at 160 °C).

3.3.3 Tunability of the fiber properties

The chemical composition of the fiber residue obtained by the one-step extraction method indicates the possibility of retaining carbohydrate composition to some degree, while extracting a part of the lignin with retained structural features, Table 5. Contrasting the fiber retrieved at a lower temperature (140 °C using 4 cycles) to the ones at a higher temperature (160 °C using 15 cycles), the properties of the fibers can be tuned while simultaneously obtaining lignin with still, to a large extent, preserved structure even at the higher temperature. The retention of some hemicelluloses on the fibers may, for instance, be interesting for increased fiber yield but also for properties. On the other hand, a more crystalline fiber can be obtained using harsher conditions.

Table 5. The relative integrated area of the carbohydrate composition of spruce wood and fiber residues at 140 °C and 160 °C using 4 and 15 cycles, respectively. Number of replicates, n=2. The number of cycles is abbreviated by the C notation.

Carbohydrate	**Spruce wood**	**Spruce, 4C, 140 °C**	**Spruce, 15C, 160 °C[1]**
	Relative area %		
Glucose	70 ± 0.070	78 ± 0.51	97 ± 0.15
Mannose	16 ± 0.056	13 ± 0.34	2.2 ± 0.098
Xylose	8.2 ± 0.010	6.6 ± 0.10	1.1 ± 0.056
Galactose	3.5 ± 0.043	1.3 ± 0.029	n.d.[1]
Arabinose	1.7 ± 0.00065	0.14 ± 0.0072	n.d.
GalA	0.86 ± 0.034	0.68 ± 0.047	n.d.
GlcA	0.094 ± 0.0045	0.05 ± 0.0015	n.d.

[1]n.d.=not detected.

The extraction temperature impacts the yield of carbohydrates and water-soluble lignin ending up in the water-soluble fraction, Figure 14. The yield of water-soluble fraction, based on total mass %, was lower at 140 °C by the 4 cycles (22%) and 9 cycles (25%) compared to the 15 cycles at 160 °C (48%). The results from the 4 + 4 cycles of 140 °C + 160 °C (by 31%) extraction also indicate the role of increasing the temperature, where the total number of cycles was 8. The temperature might explain the relatively high extractability of fragments derived from hemicelluloses, as has been observed in previous work and also substantiated in the two-step process of the present study [70, 87]. Due to the acidic environment and relatively high temperature, the hydrolysis of polysaccharides to yield monomers, dimers, and oligomers occurred and was evidenced by sugar signals in the HSQC NMR of the water-soluble part in Paper II. The crystalline part of cellulose is resistant to hydrolysis at the conditions used within the study, and the crystallinity of the fiber may increase when the amorphous part of cellulose is hydrolyzed.

The yield of the lignin and fiber fraction by the one-step extraction method was contrasted with the yield from the two-step extraction (Paper 1), Table 6. At the same extraction condition, i.e., 15C at 160°C, lignin yield was more than 10% units higher for the one-step process than for the 2-step process (c.f. 67% and 53%). This can be explained by the fact that the two-step extraction experiences some lignin losses in the hydrothermal extraction step, present as lignin moieties associated with the extracted hemicelluloses in LCCs.

Table 6. The yield trends of the lignin and fiber fractions using the one-step extraction method, including the two-step extraction method as a reference. The number of cycles is abbreviated by the C notation.

Extraction entry	**Lignin yield [mass % of wood lignin]**	**Fiber residue [% of wood mass]**
Spruce, 4C, 140 °C	19 ± 0.21[1]	74 ± 3.0
Spruce, 4C, 140+160 °C[2]	40.0	59
Spruce, 9C, 140 °C	36	65
Spruce, 15C, 160 °C	67	34
Birch, 9C, 140 °C	35	62
Two-step cyclic, spruce, 15C, 160 °C[3]	53 ± 0.79[1]	41 ± 1.6
Two-step cyclic, spruce, 15C, 140 °C[4]	30 ± 3.0[1]	58 ± 1.1

[1]Number of replicates n=3. [2]4 cycle extraction at 140 °C followed by 4 cycle extraction at 160 °C, where the lignin yield at 140 °C was 19% and at 160 °C 21%. [3]The two-step extraction method is described in Paper I. [4]The results are collected from Paper II.

Aromatic signals were observed in the HSQC spectrum of the hydrothermally extracted material (Paper I). In general, lignin yields were improved with temperature, while the opposite holds for the fiber residues. Overall, the relatively low standard deviation indicates a high repeatability of the cyclic OS extraction method, Table 6.

To summarize this part, the short one-step cyclic OS extraction was attractive as higher preservation of the lignin structure was achieved. At the same time, the carbohydrate composition was maintained in the fiber to a large extent. From a dual perspective of lignin and fiber composition, it was possible to tune the fiber properties with retained lignin quality achieved by cyclic extraction. The cyclic OS extraction method concept worked similarly for the investigated SW (spruce) and HW (birch) specie, demonstrating the cyclic OS extraction method's universality attributed to the physical protection principle. The flexibility of this process for raw material, as well as the ability to tailor the product outcome, was hereby demonstrated.

3.4 Lignin analytics: Robust characterization techniques (Paper IV)

Extracting lignin without affecting the native structure can be regarded as speculative. Lignin possesses different properties and structural features depending on several factors, including species and morphological origin, such as location in the biomass. Depending on how the lignin is extracted from biomass, new chemical properties could be introduced. The interest in using lignin for biomaterials has increased. The knowledge about molecular structure is therefore important to enable studies on structure-property relationships.

As lignin properties differ based on origin, extraction method, and sometimes batch-wise, the analytical methods may need to be optimized depending on which type of lignin is investigated. A brief introduction of selected commonly used analytical techniques for lignin analysis, by different NMR methods, SEC, and MS techniques, with or without prior chromatographic separation, is summarized below.

3.4.1 NMR characterization of lignin

NMR is a powerful tool for lignin structure analysis. Both 1-dimensional (1D) and 2-dimensional (2D) NMR techniques have been successfully used to characterize different properties of lignin derived from different sources and extraction methodologies [7, 88-91]. Semi-quantification of interunit linkages and substructures in lignin can be performed by the 2D ^{13}C-^{1}H correlation HSQC NMR experiments using the Ar-C_2 region on the lignin molecule as internal standard due to the limited substitution at this position in the native state of lignin [62]. The HSQC NMR analysis is advantageous for complex analytes such as lignin due to the separation of signals in the 2-dimensional spectra, even if it can still suffer from spectral overlaps. Combining HSQC NMR and 1D experiments can assist the signal assignments for the 1D spectrum, which otherwise often suffers from overlapping. [15, 92] ^{13}C NMR analysis of lignin is beneficial for quantitative studies. In addition, the analysis of quaternary carbons, which cannot be directly analyzed by HSQC, is achieved. Furthermore, the hydroxyl functionalities in lignin can be quantified by ^{31}P NMR by phosphorylation of the hydroxyl functionalities present on the phenol and aliphatic side-chain on the lignin molecules [60, 93]. The hydroxyl functionality has an important impact on the lignin reactivity under processing conditions. The hydroxyl groups can also be used as chemical handles through cross-linking reactions for biomaterial production [83, 84, 91]. A limitation of the discussed NMR techniques is that only the bulk is analyzed. For the differentiation of populations, other techniques need to be considered.

3.4.2 SEC analysis of lignin

Determining the molecular weight of lignin has been a debated topic with several challenges. Size exclusion chromatography (SEC) is commonly used in combination with UV/RI detection and linear standards such as polystyrene [65]. In the view of developing methods suitable for lignin analysis and towards more accurate results, the standard should match the properties of the lignin of interest, which might differ depending on how it was retrieved from the biomass. It is understandable that 1) the same standards may not be used for all types of lignin, and 2) the knowledge about the conformation in the chromatographic solvent should be considered since the measurement is based on the hydrodynamic radius. To address the solubility challenge, using THF-SEC systems, the lignin samples are often acetylated to enhance the solubility [65], where the hydroxyl functionalities are acetylated to decrease the polarity of the lignin sample. However, the molar mass changes to a certain degree by acetylation. To address some of these issues, multi-angle light scattering (MALS) detection is reported. Here, the relationship between the intensity of the scattered light is correlated with the molar mass of the lignin molecules with no necessity of lignin standards [94, 95].

3.4.3 MS for lignin

Due to challenges with the determination of the molecular weight of lignin using SEC, which was discussed in *section 3.4.2*, trials have been reported where matrix-assisted laser desorption/ionization (MALDI) mass spectrometry (MS) was used in combination with SEC for the determination of the absolute average molar mass of lignin. [96] MALDI is a soft ionization technique that can potentially be used as an ion source in MS to analyze lignin with limited effect on the structural integrity of the molecules during ionization [97]. The matrix is involved in the ionization of analytes, where the matrix absorbs the energy from the laser irradiation and ionizes the analytes. MALDI ionization is often used with the mass analyzer Time-of-Flight (TOF) to separate the generated ions in the flight tube by the mass-to-charge ratio [98]. The analysis can be done with or without a matrix, and unlike many other analysis techniques and methods, for MALDI, the analyte does not have to be soluble in the matrix solution, which might be beneficial for complex samples [99]. Hypothetically, the MALDI ionization technique has an advantage for lignin analysis due to the inherent complexity of lignin by functionalities and heterogeneity and has been used to investigate lignin polymerization [100]. As with many analytical techniques, there are limitations of MALDI that have been discussed, including the formation of inhomogeneous matrix mixtures through the immiscibility of matrix and substrate and low ionization efficiency [101]. Different matrices have been evaluated in both positive and negative modes for lignin analysis, where the 2,5-dihydrobenzoic acid (2,5-DHB) has been commonly used [102]. The selection of the matrix might affect which part of the sample is detected, and novel matrices, such as a matrix based on ionic liquids, have been evaluated to overcome limitations in lignin analysis, such as improvement of ionization efficiency [101, 103].

Other MS analyses with or without preceding chromatography separation have been evaluated using both single MS and tandem MS (MS/MS) to investigate both sequencings in lignin polymerization and to identify oligomeric fractions of different technical lignins [104-109].

3.4.4 Investigation of lignin structures by combinations of techniques

There is a need for robust analytical techniques and suitable methods to analyze lignin. The complexity of lignin limits the evaluation of the properties, which needs further investigation. The limitations of the different analytical techniques have been briefly discussed in *sections 3.4.1-3.4.3*. By combining the results obtained from different techniques, more in-depth knowledge of the lignin characteristics can be obtained. Using the combination of NMR methods and MALDI-TOF MS, the populations and sequences of lignin linkages could be further investigated. Additionally, by combining information from the different analytical techniques, the theories of lignin reaction during OS extraction could be discussed, with support from computational modeling and DFT calculations.

The substrates studied were the cyclic extracted organosolv lignin (two-step process) and a bio-mimic lignin reference synthesized in accordance with the literature [110-112]. Separation of the crude bio-mimic lignin product into dimers and oligomeric fractions was done by column chromatography using silica. The ethanol-soluble part of the two-step cyclic OS extraction of lignin obtained at 160 °C, presented in *section 3.1.1*, was used in the analyses as an extracted lignin representative. The fraction corresponds to approximately 46% of the extracted lignin fraction with a Đ of 1.8, M_n of 1100 g/mol, and a DP_n of 6 units, analyzed by SEC (THF system).

The ethanol-soluble cyclic OS lignin was first used to screen for suitable matrices, diluents, and possible additives in both positive and negative modes. The lignin sample was expected to have higher complexity than the synthesized reference sample and, thereby, was regarded to be more challenging to analyze. The matrix solutions were evaluated by the number of signals in the regions expected for oligomeric lignin substrates. The best result was obtained using DMSO as a diluent and 2,5-DHB in TA30 as a matrix, recorded in positive mode. The optimized method was selected for further analysis of lignin and the synthesized reference sample within the study.

3.4.5 Analysis of reference bio-mimic lignin

The dimers and oligomeric fractions of the synthesized lignin reference were analyzed by MALDI-TOF MS and HSQC NMR. The results from both analytical techniques were in agreement. More specifically, the most common dimers, i.e., the ones with β-O-4′, β-β′and β-5′ interunit linkages, were detected by both methods. Furthermore, the β-O-4′ was by far the most abundant interunit in the oligomeric fraction. Dimers were assigned from the MALDI-TOF MS analysis based on the respective sodium and potassium adduct cations. The recorded monoisotopic *m/z* of the sodium adducts of the dimers together with the calculated monoisotopic *m/z* in parentheses was as follows; β-O-4′: *m/z* 399.35 (*m/z* 399.14), β-5′: *m/z* 381.37 (*m/z* 381.13) and β-β′: *m/z* 381.37 (*m/z* 381.13).

The MALDI-TOF MS analysis of the oligomeric fractions revealed the presence of uniformly distanced clusters representing a region consisting of trimers to octamers, Figure 20 (I). From the HSQC analysis of the oligomeric reference fraction, a β-O-4′ content of around 50% was estimated. This is close to what has been proposed for native spruce lignin [6]. The oligomers were formed by the same mechanistic principles described by the radical couplings of CA-OH to preformed dimer radicals in an endwise polymerization. This was evident from the mass increments of 178 and 196 observed in MS, corresponding to the formations of β-β′/β-5′ and β-O-4′, respectively. The mass increment of 180 was not a radical coupling but rather an addition reaction of coniferyl alcohol to a preformed quinone methide intermediate, typically in a β-O-4′ sub-structure, Figure 20. This reaction yields either an α-O-4′ linkage or an γ-O-α′ linkage, both in a β-O-4′ structure. The detection of these structures conveys the introduction of branching points into the growing lignin chain, for this system, at the tetrameric stage, Figure 20 (II). It is worth noting that this may not occur in truly native environments. However, the possibility cannot be written out given that several cell types exist and the environments in which they exist are tuned to serve specific functions. The sequence of reactions described for the tetramers also formed pentamers in the cluster region around *m/z* 900, Figure 20, up to octamers in the region around *m/z* 1450.

I

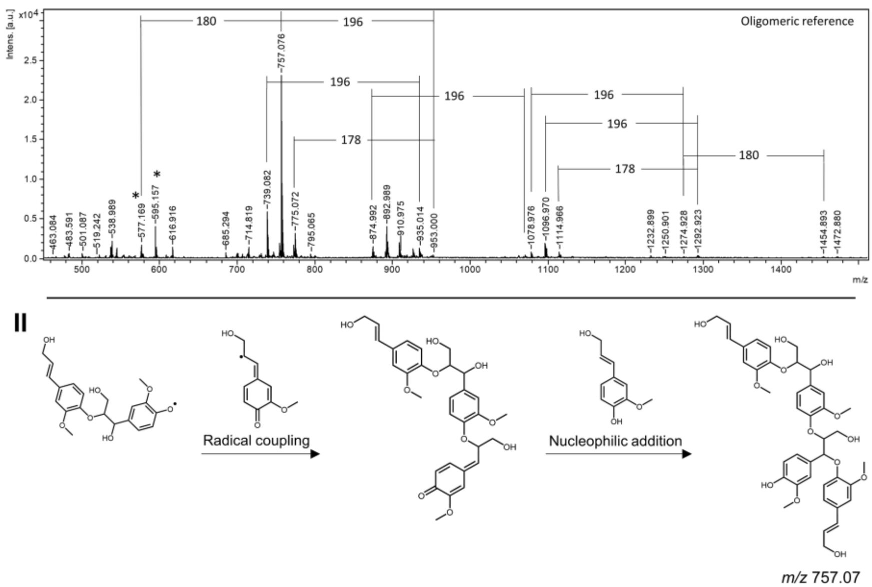

Figure 20. MALDI-TOF MS spectrum of the oligomeric reference bio-mimic lignin (I) and example of the formation of benzylic ether with measured monoisotopic *m/z* 757.07 with the calculated monoisotopic *m/z* 757.28 (II).

3.4.6 Physical protected lignin: structural populations

Analysis of the ethanol-soluble fraction of the two-step cyclic OS method (*section 3.1.1*) by HSQC NMR gave a β-O-4′ content of 30%, a β-5′ of 12%, and a β-β′ of 2%. The aliphatic and phenolic hydroxyls, studied by ^{31}P NMR, were quantified at 3.1 mmol/g and 2.2 mmol/g lignin, respectively. Other interunit linkages related to OS-extracted lignin, Figure 7, were identified in an amount similar to already reported values, Table 1 (*section 3.1.1*).

The same lignin was analyzed by MALDI-TOF MS in positive mode according to the selected method, *section 3.4.4*. The *m/z* of approximately 1700, Figure 21, indicates that the largest population consists of roughly eight lignin monomer units. Similar to the bio-mimic lignin reference, Figure 20, a pattern of clusters could be identified, Figure 21. Unlike the bio-mimic lignin, where the polymerization could be followed by cluster analyses, the cluster analysis of the ethanol-soluble lignin indicated the fragmentation of the lignin oligomers. The fragmentation most likely occurred during the acidic OS extraction.

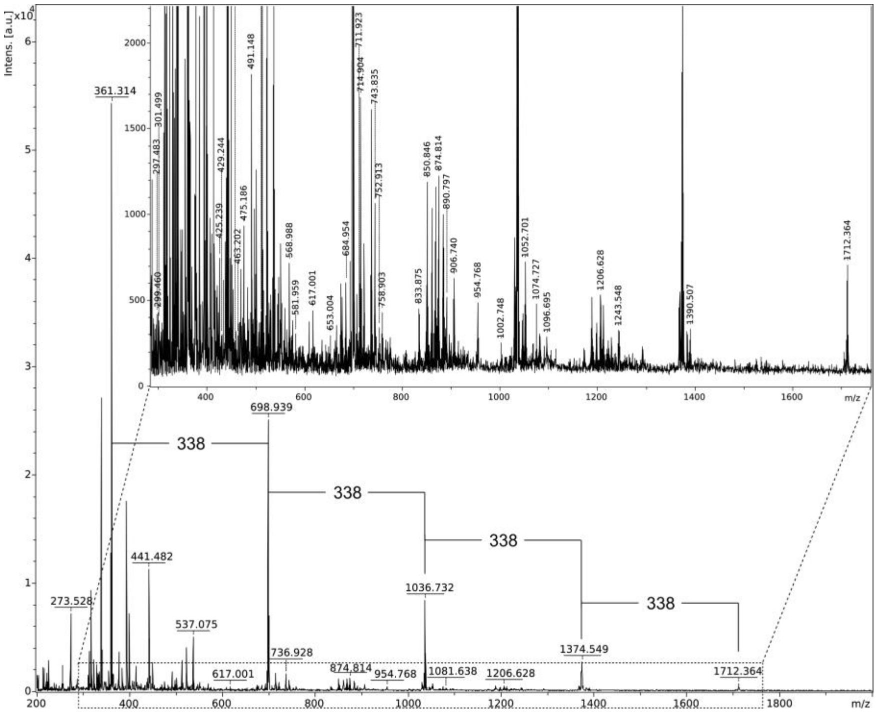

Figure 21. MALDI-TOF MS spectrum of the ethanol-soluble lignin fraction from the two-step OS extraction method obtained at 160 °C. Figure adapted from Paper IV [113] with permission from the American Chemical Society.

The pattern of clusters has also been shown in other works of lignin analysis by MALDI-TOF MS [100, 114]. In this study, however, the cluster analysis suggests a mass increment 338 Da, likely a dimeric repeating unit that has lost small molecules from the sidechain. This assumption was based on the fact that unmodified dimeric units/segments in lignin would have a mass in the range of 360-392 Da. The loss yielding 338 could originate, for instance, from the formation of benzylic cations during the acidic OS extraction, which could be followed by intramolecular condensation reactions [114].

Two tentative structures with respective formation mechanisms were proposed based on the mass difference of 338 Da, Figure 22. Due to the regularity of the repeating units, the dimeric units were proposed to originate from an octameric β-O-4′ of lignin, Figure 22 (A) or a tetrameric structure consisting of alternating interunit connections (B). Noteworthy is that the terms octameric and tetrameric are defined here based on the repeating units. In case A, eight monolignols were connected by β-O-4′, hence the term octameric. In case B, each repeating unit consists of β-O-4′ and β-5′, and there were four such units. Hence the term tetrameric is used for B. Note that both the alternatives (A and B) consist of 8 aromatic rings.

A possible explanation of how these tentative structures were formed now follows. At acid-catalyzed OS extraction conditions, the benzylic carbocation on the α-position reacts to form an intramolecular condensation resulting in α-5′ connection, also illustrated in Figure 3 and Figure 22 (I), and reported in other work [32, 114]. This internal capping does not cause an increase in molecular weight or recalcitrance as otherwise might be expected for similar intermolecular condensations [115, 116]. During the MALDI ionization step, methanol might be lost [114], likely due to heterolytic cleavage caused by laser ablation. The formed carbocation loses a proton to form the unsaturated coumaran structure, Figure 22 (I, MALDI events). This was followed by a series of oxidation reactions forming ketone and aldehyde functionalities on the lignin molecule. The oxidation of the lignin structure can be initiated from hydroxyl radicals that are possibly formed by the laser irradiation of the 2,5-DHB matrix [117] with the formation of carbonyl functionalities on the lignin molecules and formation of water and molecular hydrogen, Figure 22 (A, I).

The alternating β-O-4′ and β-5′ structures, Figure 22 (II), react based on similar mechanistic principles described for (I, A). The β-5′ structure may undergo methanol and proton loss under the MALDI events. The aliphatic hydroxyls oxidized by the hydroxy radicals from the irradiated matrix to carbonyls yield ketones and aldehydes functionalities on the lignin molecule, Figure 22 (II, B).

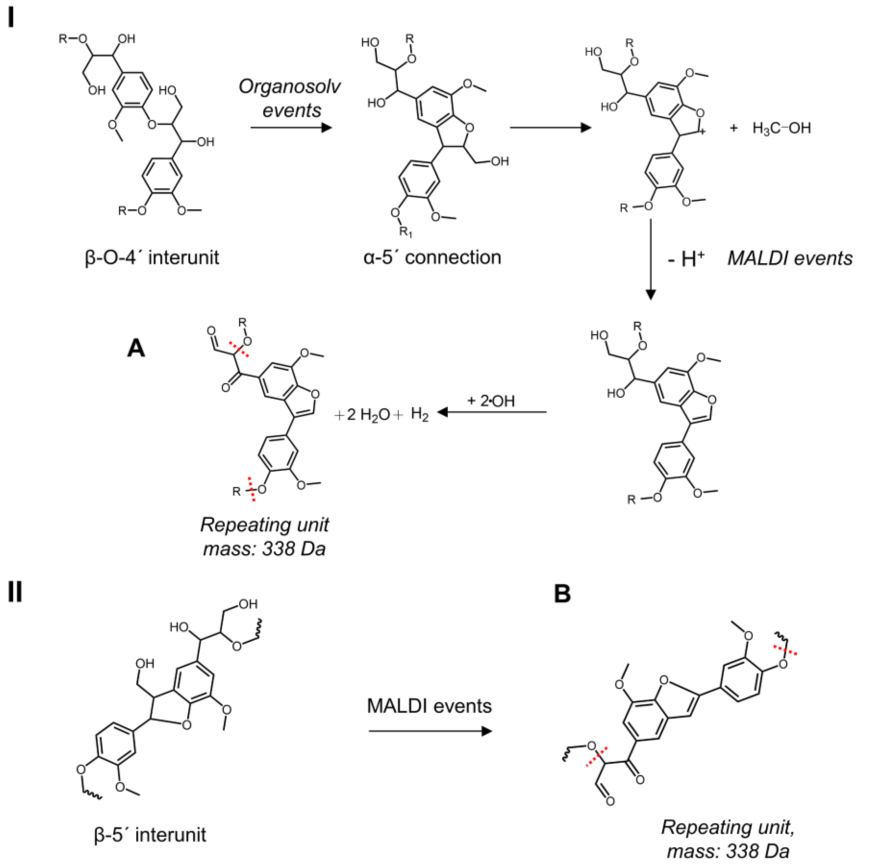

Figure 22. Tentative structures analyzed by MALDI-TOF MS illustrating two possible pathways for the formation of lignin units of 338 Da, by the β-O-4′ backbone (A) and the altering of β-O-4′ and β-5′ interunit (B). The red lines indicate the boundaries of the repeating units of 338 Da.

Interestingly for the reaction system in (I), Figure 22, the formation of intramolecular α-5′ connections seems to occur at every second β-O-4′ structure on the backbone. An explanation of this alternate condensation occurrence was derived from DFT modeling. The β-O-4′ interunit linkages are flexible and can fold to form π-π stackings in the form of sandwich and T-shaped stackings, which was also shown in the DFT modeling of β-O-4′ hexamers (Paper IV). The occurrence of π-π stackings in lignin has been reported earlier for native and processed lignin [118, 119]. The distance between the π-π stackings depends on the stiffness of the molecular units and conformation, with a shorter distance for sandwich stackings compared to T-shaped stackings (Paper IV). The modeled β-O-4′ hexamers had a spiral shape, showing closer proximity to the benzylic C_α and Ar-C_5 for sandwich π-π stackings when compared to the T-shaped π-π stackings. This provided a plausible explanation for the proposed formation of the alternating α-5′ intramolecular condensations, where sandwich stacked rings can undergo the reaction due to distances between reactive sites being close enough, while T-shaped cannot.

To summarize this part, MALDI-TOF MS analysis was shown to be a promising complement to NMR techniques for lignin analysis. DFT calculations were essential for explaining the selectivity of condensation reactions during the extraction. The MALDI-TOF MS analysis of the bio-mimicked lignin enabled studies on lignin polymerization sequences. The polymerization occurred in an endwise fashion, and the emergence of an etherified branching point at the benzylic carbon in β-O-4′ substructures was shown. Due to the earlier discussed shortcomings of MALDI-TOF MS analysis, *section 3.4.3*, the results should not be seen as representative for the whole lignin sample, but still, studies of partial populations can be obtained. Further investigation into lignin analysis by MALDI MS and other MS-related techniques might contribute to understanding the discrimination of the ionization of lignin analytes.

3.5 Lignin for biobased applications

Having developed a process concept where lignin with preserved structures was obtained, it was relevant to test its applicability with respect to benchmark technical lignins. Using lignin for different biobased applications is of high interest in the transition toward a biobased society. Lignin has been proposed and tested for applications such as composites and adhesives [120, 121]. A field of increasing attention is the utilization of lignin nanoparticles (LNPs) for biobased applications such as cosmetics, packaging, and food additives, where the properties of lignin, such as UV barrier and radical scavenger, are of special interest [122-125]. As previously discussed, OS-extracted and technical lignin, such as kraft lignin, suffer from heterogeneity due to severe alteration of the native lignin structures caused by the process conditions [41, 43]. The kraft process [126] is the most commonly used pulping process at present. Several approaches have been developed to retrieve the lignin from the black liquor to obtain the product generally termed kraft lignin. One such process is the LignoBoost process [127]. As illustrated in Figure 17, *section 3.3.2,* less than 50% of the interunit linkages in the kraft lignin are known. This is problematic from a user perspective since the structure-property relationships cannot be properly evaluated. Furthermore, the controlled synthesis of high-quality materials benefits from complete knowledge of the structure of the precursor and the capability to follow the chemistry through the synthetic steps. With this background, lignin derived from different extraction processes was evaluated to produce LNPs in Paper V, focusing mainly on lignin properties. Even though the structure of kraft lignin is still poorly known, left with few options, kraft, and batch-organosolv lignin were used as benchmarks for the protected organosolv lignin in the fundamental study on LNPs.

3.5.1 Lignin properties behind LNPs

The investigation concerned how different lignin sources affect the properties of lignin nanoparticles (LNPs). For this purpose, lignin derived from different processes was used as substrates; LignoBoost lignin (kraft), Alcell-based OS lignin (OS reference), and lignin derived by the two-step extraction method (OS protected) described in *section 3.1.1*. All crude lignins were ethanol fractionated to decrease the Đ and further characterized by HSQC NMR, ^{31}P NMR, and SEC to identify the chemical and physical properties of the lignins. The lignin fractions derived from different processes had a similar M_n in the range of 800-1100 g/mol. The similarities in M_n qualified these fractions for the study on the effect of lignin structure on the LNP properties, given that the results would be devoid of interference effects from molar mass differences. Generally, the size of LNPs is suggested to decrease by an increased molecular weight of lignin due to higher hydrophobicity and faster nucleation for the higher molecular weight lignin [128, 129]. However, within this study, the size of LNPs was found to be different irrespective of similar molecular weight, which pointed toward effects from different molecular structures.

Based on the structural analysis (I and II in Figure 23, more details in Paper V), structural motifs for the three lignins were introduced, Figure 24, and used in DFT modeling to further investigate the role of lignin structure in the properties of LNPs. The hypothesis was that the structural conformation of lignin molecules might play important roles in the assembly process to form LNPs with different properties, such as LNP sizes, surface morphology and functionality. In Figure 23, the quantified interunit linkages and substructures (I), aliphatic and phenolic hydroxyl content (II), and molecular size distribution (III) are illustrated.

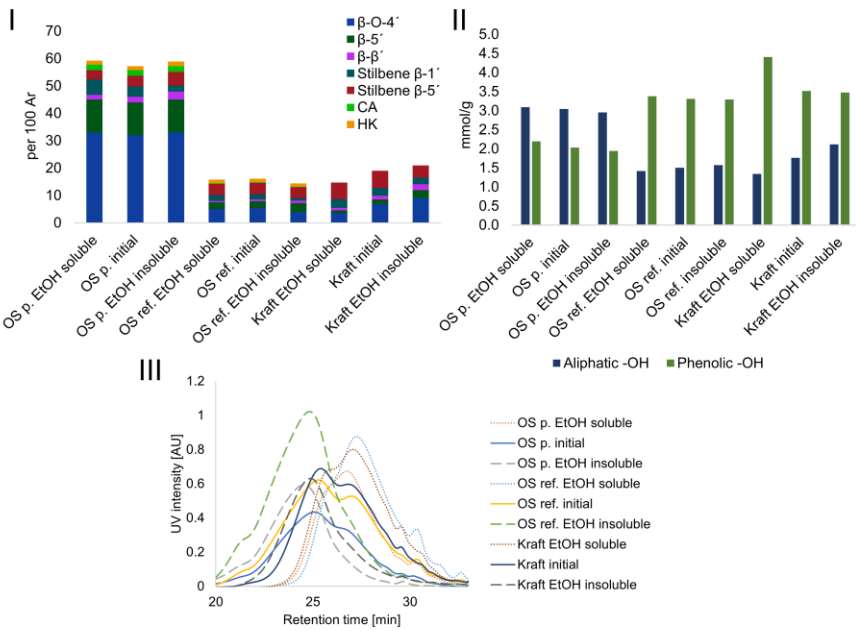

Figure 23. Content of interunit linkages and substructures (I), quantification of aliphatic and phenolic hydroxyl functionalities (II), and molecular size distribution (III).

The surface properties of the LNPs were characterized by liquid-state ^{1}H NMR, using earlier reported methods for surface characterization of LNPs in D_2O [130]. The presence of non-oxygenated aliphatic units on the surface of the LNPs was more pronounced for the OS protected lignin when compared to the kraft and OS reference lignin, where methoxy and aromatic protons were more prevalent (Paper V, Figure 6). Structural models of the ethanol-soluble fractions, representing around 50% of the lignin fractions, were proposed based on the HSQC NMR, ^{31}P NMR and SEC analysis, Figure 24, and used as input for the DFT conformational modeling.

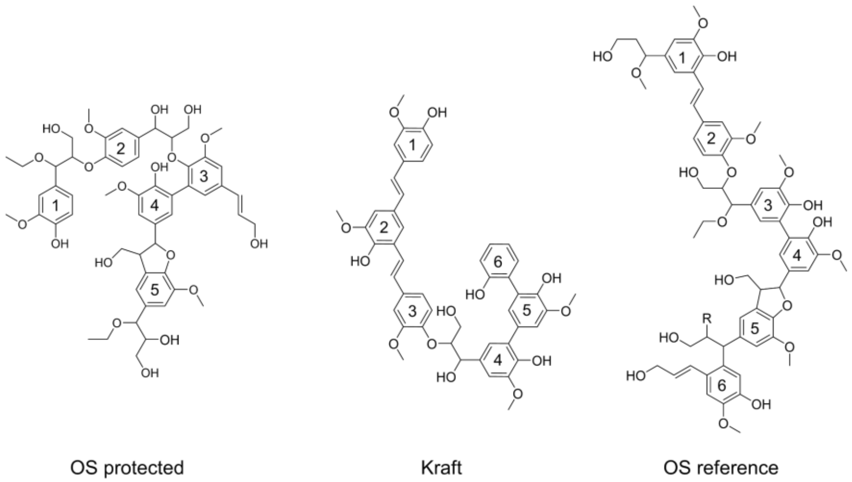

Figure 24. Structures of the lignins based on HSQC NMR, ^{31}P NMR and SEC analysis with a molecular weight in the range of approximately 800-1100 Da.

The DFT modeling showed that the types of interunit linkages, combined with the linkage sequence, yielded, as expected, different molecular configurations (Paper V, Figure 5). However, the impact of flexible β-O-4′ bonds was noteworthy, causing molecular folding and an overall folded shape as a result of intramolecular π-π stacking. For instance, for the OS protected lignin, intramolecular T-shaped π-π stacking (between the aromatic ring 1-2 and 2-3, Figure 24) based on the presence of two adjacent β-O-4′ structures in the molecule was identified. The OS reference and kraft lignin formed sandwich π-π stacking (between the aromatic ring 3-4 for kraft and 2-3 for OS reference, Figure 24) introduced by the single β-O-4′ bond in the respective molecules. Overall, the DFT modeling indicated that the conformation of lignin molecules and the type of intramolecular interactions were affected by the chemical structure of the lignin. The volumes of the resultant molecular models were different due to the structural effects on conformations (Paper V, Figure 5) and were found to correlate with the LNP sizes. Accordingly, the molecular model of the protected and reference organosolv lignin showed a larger volume than the kraft lignin and produced larger LNPs than the kraft lignin (details in Paper V). The higher content of oxygenated aliphatic side groups in the organosolv lignin, when compared to the kraft lignin with proposed higher aromatic density, might explain this trend. The combination of chemical analysis and DFT modeling indicates that the properties of the LNPs were affected by the nature of the lignin precursor on a structural level.

4 Conclusions and prospects

The investigations on utilizing lignin as a replacement for fossil resources have gained momentum due to the quest to transition toward a more sustainable society. A major challenge to this progress is that available lignins suffer from poorly known properties, most notably the molecular structure.

Grounded on fundamental knowledge, a biorefinery concept to procure lignin with a protected structure and preserved integrity was developed in this work. The concept was based on the physical protection of lignin structure, which was achieved through cyclic extraction.

Investigations of the cyclic extractions by chemometrics and design of experiment (DoE) approaches demonstrated the possibility of fine-tuning the lignin properties with retained structural integrity.

Further development of the process was achieved by reducing process steps, which is beneficial from the viewpoint of chemical usage, recovery, and recyclability. This was shown to improve both lignin yield and structure preservation. It was also shown that the properties of the residual fibers could be tailored by process pathway selection, i.e., two-step versus one-step. In the former case, a more crystalline fiber was obtained, while in the latter, more hemicelluloses were retained.

Overall, the structural accountability of the cyclic extracted lignin was superior to that of benchmark technical lignins, as demonstrated by NMR and MALDI-TOF MS analysis. This study demonstrates the important role of fundamental investigations, at a molecular level, in tailored lignin biorefining and will inform lignin valorization efforts. In this context, further development of lignin analytics will be essential.

5 Acknowledgements

First, I would like to acknowledge Knut and Alice Wallenberg foundation through the Wallenberg Wood Science Center for founding this PhD project.

I want to express my gratitude to my principal supervisor Prof. Martin Lawoko, who let me into the group. I have appreciated the support, interesting discussions, and friendship during these four years. It has been a great pleasure to work with you.

My co-supervisor Prof. Åsa Emmer for letting me work in your lab and for all the support and fruitful discussions regarding analytical chemistry. Dr. Olena Sevastyanova for support and discussions.

I would like to express my acknowledgment to all my co-authors and collaborators: Pär, Nicola, Vijaya, Raghu, Joakim, Thomas, Ievgen, Barbara, Isabella, Monica, and Jenevieve. Thank you all for the very nice collaborations.

A special thanks to my colleagues at WWSC in Stockholm and around Sweden for the wonderful moments we have spent together at different events and in the office and lab. To name a few, Isabella and Rebecca, for all the fun we had during this time. Also, Iuliana, Poornima, Martin, Luna, Lars, and others in the WWSC community, for your friendship and all the interesting discussions. I also want to acknowledge Gunnar Westman and Paul Gatenholm for arranging the amazing winter and summer schools.

I want to thank my colleagues and friends at the Department of Fibre and Polymer Technology and in the Wood Chemistry and Pulp Technology division. You have created a nice atmosphere and made work enjoyable.

Finally, I want to thank my lovely children, Svea and Gustav, for being my sunshine and inspiration in life! I would also like to thank my family and Anders for all your support during this journey.

6 References

1. Bruijnincx, P.C. and B.M. Weckhuysen, *Lignin up for break-down*. Nature chemistry, 2014. **6**(12): p. 1035-1036.
2. Adler, E., *Lignin chemistry—past, present and future*. Wood science and technology, 1977. **11**(3): p. 169-218.
3. White, R.H., *Effect of lignin content and extractives on the higher heating value of wood*. Wood and fiber science, 1987: p. 446-452.
4. Fengel, D. and G. Wegener, *Wood: chemistry, ultrastructure, reactions*. 2011: Walter de Gruyter.
5. Xu, C., et al., *Lignin depolymerisation strategies: towards valuable chemicals and fuels*. Chemical Society Reviews, 2014. **43**(22): p. 7485-7500.
6. Ralph, J., C. Lapierre, and W. Boerjan, *Lignin structure and its engineering*. Current opinion in biotechnology, 2019. **56**: p. 240-249.
7. Balakshin, M., et al., *Spruce milled wood lignin: linear, branched or cross-linked?* Green Chemistry, 2020. **22**(13): p. 3985-4001.
8. Boerjan, W., J. Ralph, and M. Baucher, *Lignin biosynthesis*. Annual review of plant biology, 2003. **54**(1): p. 519-546.
9. Lin, S.Y. and C.W. Dence, *Methods in lignin chemistry*. 2012: Springer Science & Business Media.
10. Fergus, B., et al., *The distribution of lignin in sprucewood as determined by ultraviolet microscopy*. Wood Science and Technology, 1969. **3**: p. 117-138.
11. Fergus, B. and D. Goring, *The distribution of lignin in birch wood as determined by ultraviolet microscopy*. Holzforschung, 1970. **24**: p. 118-124.
12. Ralph, J., et al., *Lignins: natural polymers from oxidative coupling of 4-hydroxyphenyl-propanoids*. Phytochemistry reviews, 2004. **3**: p. 29-60.
13. Vanholme, R., et al., *Metabolic engineering of novel lignin in biomass crops*. New Phytologist, 2012. **196**(4): p. 978-1000.
14. Zhao, W., et al., *From lignin subunits to aggregates: insights into lignin solubilization*. Green Chemistry, 2017. **19**(14): p. 3272-3281.
15. Giummarella, N., et al., *Structural features of mildly fractionated lignin carbohydrate complexes (LCC) from spruce*. Rsc Advances, 2016. **6**(48): p. 42120-42131.
16. Vermaas, J.V., M.F. Crowley, and G.T. Beckham, *A quantitative molecular atlas for interactions between lignin and cellulose*. ACS

Sustainable Chemistry & Engineering, 2019. **7**(24): p. 19570-19583.
17. Kang, X., et al., *Lignin-polysaccharide interactions in plant secondary cell walls revealed by solid-state NMR*. Nature communications, 2019. **10**(1): p. 347.
18. Kleinert, T.N., *(Pointe Claire, Quebec, CA), US3585104A*. US3585104A, 1971.
19. Johansson, A., O. Aaltonen, and P. Ylinen, *Organosolv pulping—methods and pulp properties*. Biomass, 1987. **13**(1): p. 45-65.
20. Kleinert, T.N. and K. TN, *Organosolv pulping with aqueous alcohol*. 1974.
21. Pye, E.K. and J.H. Lora, *The AlcellTM process: a proven alternative to kraft pulping*. Tappi journal, 1991. **74**(3): p. 113-118.
22. Young, R.A. and M. Akhtar, *Environmentally friendly technologies for the pulp and paper industry*. 1997: John Wiley & Sons.
23. Diebold VB, C.W., Walsh, JK. , *Solvent pulping process.* , C.P.A. Ltd, Editor. 1978: US.
24. Liu, Y., et al., *A Comparison of the Structural Changes Occurring in Lignin during Alcell and Kraft Pulping of Hardwoods and Softwoods*, in *Lignin: Historical, Biological, and Materials Perspectives*. 1999, American Chemical Society. p. 447-464.
25. Graglia, M., N. Kanna, and D. Esposito, *Lignin refinery: Towards the preparation of renewable aromatic building blocks*. ChemBioEng Reviews, 2015. **2**(6): p. 377-392.
26. de la Torre, M.J., et al., *Organosolv lignin for biofuel.* Industrial crops and products, 2013. **45**: p. 58-63.
27. Shimada, K., S. Hosoya, and T. Ikeda, *Condensation reactions of softwood and hardwood lignin model compounds under organic acid cooking conditions*. Journal of wood chemistry and technology, 1997. **17**(1-2): p. 57-72.
28. Berlin, A. and M. Balakshin, *Industrial lignins: analysis, properties, and applications*. Bioenergy research: advances and applications, 2014: p. 315-336.
29. Fisher, H.E., M. Kulka, and H. Hibbert, *Studies on Lignin and Related Compounds. LXXIX. Synthesis and Properties of 3-Hydroxy-1-(3, 4-dimethoxyphenyl)-2-propanone1*. Journal of the American Chemical Society, 1944. **66**(4): p. 598-601.
30. Miles-Barrett, D.M., et al., *The synthesis and analysis of lignin-bound Hibbert ketone structures in technical lignins*. Organic & Biomolecular Chemistry, 2016. **14**(42): p. 10023-10030.

31. De Gregorio, G.F., et al., *Mechanistic insights into lignin depolymerisation in acidic ionic liquids*. Green Chemistry, 2016. **18**(20): p. 5456-5465.
32. Bauer, S., et al., *Characterization of Miscanthus giganteus lignin isolated by ethanol organosolv process under reflux condition*. Journal of agricultural and food chemistry, 2012. **60**(33): p. 8203-8212.
33. Li, S., K. Lundquist, and U. Westermark, *Cleavage of arylglycerol β-aryl ethers under neutral and acid conditions*. Nordic Pulp & Paper Research Journal, 2000. **15**(4): p. 292-299.
34. Westermark, U., B. Samuelsson, and K. Lundquist, *Homolytic cleavage of the β-ether bond in phenolic β-O-4 structures in wood lignin and in guaiacylglycerol-β-guaiacyl ether*. Research on chemical intermediates, 1995. **21**(3-5): p. 343-352.
35. Sturgeon, M.R., et al., *A mechanistic investigation of acid-catalyzed cleavage of aryl-ether linkages: implications for lignin depolymerization in acidic environments*. ACS Sustainable Chemistry & Engineering, 2014. **2**(3): p. 472-485.
36. Lourencon, T.V., et al., *Lignin-First Integrated Hydrothermal Treatment (HTT) and Synthesis of Low-Cost Biorefinery Particles*. ACS Sustainable Chemistry & Engineering, 2020. **8**(2): p. 1230-1239.
37. Kobayashi, T., et al., *Molecular-level consequences of biomass pretreatment by dilute sulfuric acid at various temperatures*. Energy & Fuels, 2011. **25**(4): p. 1790-1797.
38. Cao, S., et al., *Chemical transformations of Populus trichocarpa during dilute acid pretreatment*. Rsc Advances, 2012. **2**(29): p. 10925-10936.
39. Nimz, H., *A new type of rearrangement in the lignin field*. Angewandte Chemie International Edition in English, 1966. **5**(9): p. 843-843.
40. Li, J. and G. Gellerstedt, *Improved lignin properties and reactivity by modifications in the autohydrolysis process of aspen wood*. Industrial crops and products, 2008. **27**(2): p. 175-181.
41. Chakar, F.S. and A.J. Ragauskas, *Review of current and future softwood kraft lignin process chemistry*. Industrial Crops and Products, 2004. **20**(2): p. 131-141.
42. Giummarella, N., et al., *Fractional profiling of kraft lignin structure: Unravelling insights on lignin reaction mechanisms*. ACS Sustainable Chemistry & Engineering, 2019. **8**(2): p. 1112-1120.

43. Crestini, C., et al., *On the structure of softwood kraft lignin*. Green Chemistry, 2017. **19**(17): p. 4104-4121.
44. Luo, X., et al., *Protection strategies enable selective conversion of biomass*. Angewandte Chemie International Edition, 2020. **59**(29): p. 11704-11716.
45. Shuai, L., et al., *Formaldehyde stabilization facilitates lignin monomer production during biomass depolymerization*. Science, 2016. **354**(6310): p. 329-333.
46. Lan, W., et al., *Protection group effects during α, γ-diol lignin stabilization promote high-selectivity monomer production*. Angewandte Chemie, 2018. **130**(5): p. 1370-1374.
47. Vendamme, R., et al., *Aldehyde-Assisted Lignocellulose Fractionation Provides Unique Lignin Oligomers for the Design of Tunable Polyurethane Bioresins*. Biomacromolecules, 2020. **21**(10): p. 4135-4148.
48. Deuss, P.J., et al., *Aromatic monomers by in situ conversion of reactive intermediates in the acid-catalyzed depolymerization of lignin*. Journal of the American Chemical Society, 2015. **137**(23): p. 7456-7467.
49. Lahive, C.W., et al., *Advanced model compounds for understanding acid-catalyzed lignin depolymerization: identification of renewable aromatics and a lignin-derived solvent*. Journal of the American Chemical Society, 2016. **138**(28): p. 8900-8911.
50. Zijlstra, D.S., et al., *Highly efficient semi-continuous extraction and in-line purification of high β-O-4 butanosolv lignin*. Frontiers in chemistry, 2021. **9**: p. 329.
51. Li, Y., et al., *Kinetic and mechanistic insights into hydrogenolysis of lignin to monomers in a continuous flow reactor*. Green Chemistry, 2019. **21**(13): p. 3561-3572.
52. Anderson, E.M., et al., *Flowthrough reductive catalytic fractionation of biomass*. 2017. **1**(3): p. 613-622.
53. Kumaniaev, I., et al., *Lignin depolymerization to monophenolic compounds in a flow-through system*. 2017. **19**(24): p. 5767-5771.
54. Zijlstra, D.S., et al., *Efficient mild organosolv lignin extraction in a flow-through setup yielding lignin with high β-O-4 content*. Polymers, 2019. **11**(12): p. 1913.
55. Capolupo, L. and V. Faraco, *Green methods of lignocellulose pretreatment for biorefinery development*. Applied Microbiology and Biotechnology, 2016. **100**(22): p. 9451-9467.
56. Galbe, M. and O. Wallberg, *Pretreatment for biorefineries: A review of common methods for efficient utilisation of*

lignocellulosic materials. Biotechnology for biofuels, 2019. **12**(1): p. 1-26.
57. de Jong, E. and G. Jungmeier, *Biorefinery concepts in comparison to petrochemical refineries*, in *Industrial biorefineries & white biotechnology*. 2015, Elsevier. p. 3-33.
58. Cf, O., *Transforming our world: the 2030 Agenda for Sustainable Development*. United Nations: New York, NY, USA, 2015.
59. Bozell, J.J. and M.K. Patel, *Feedstocks for the Future*. 2006: American Chemical Society Washington, DC.
60. Argyropoulos, D., *31 P NMR in wood chemistry: A review of recent progress*. Research on Chemical Intermediates, 1995. **21**(3-5): p. 373.
61. Granata, A. and D.S. Argyropoulos, *2-Chloro-4, 4, 5, 5-tetramethyl-1, 3, 2-dioxaphospholane, a reagent for the accurate determination of the uncondensed and condensed phenolic moieties in lignins*. Journal of Agricultural and Food Chemistry, 1995. **43**(6): p. 1538-1544.
62. Sette, M., R. Wechselberger, and C. Crestini, *Elucidation of lignin structure by quantitative 2D NMR*. Chemistry–A European Journal, 2011. **17**(34): p. 9529-9535.
63. Gellerstedt, G., et al., *Quantitative 13C NMR analysis of kraft lignins*. Acta Chem. Scand. B, 1987. **41**(7): p. 541-546.
64. Chen, C.-L., *Characterization of milled wood lignins and dehydrogenative polymerisates from monolignols by carbon-13 NMR spectroscopy*. 1998, ACS Publications.
65. Gellerstedt, G., *Gel permeation chromatography*, in *Methods in lignin chemistry*. 1992, Springer. p. 487-497.
66. SCAN, *Carbohydrate composition*. 2009, SCAN-CM 71:09 Scandinavian Pulp, Paper and Board testing Committee, Stockholm, Sweden.
67. TAPPI T 222 om-02, *Acid-insoluble lignin in wood and pulp*. 2002, TAPPI Test Methods, Tappi Press, Atlanta, GA, USA.
68. TAPPI UM 250, *Acid-soluble lignin in wood and pulp*. 1991, TAPPI Useful Methods, 1991, Tappi, Atlanta, GA, USA.
69. Azhar, S., et al., *Extraction of hemicelluloses from fiberized spruce wood*. Carbohydrate polymers, 2015. **117**: p. 19-24.
70. Giummarella, N. and M. Lawoko, *Structural Insights on Recalcitrance during Hydrothermal Hemicellulose Extraction from Wood*. ACS Sustainable Chemistry & Engineering, 2017. **5**(6): p. 5156-5165.

71. Li, J., G. Henriksson, and G. Gellerstedt, *Carbohydrate reactions during high-temperature steam treatment of aspen wood*. Applied biochemistry and biotechnology, 2005. **125**: p. 175-188.
72. ZHANG, L. and G. GELLERSTEDT. *Achieving quantitative assignment of lignin structure by combining 13C and HSQC NMR techniques*. in *Sixth European workshop on lignocellulosics and pulp: advances in lignocellulosics chemistry towards high quality processes and products (Bordeaux)*. 2000.
73. Leardi, R., *Experimental design in chemistry: A tutorial*. Analytica Chimica Acta, 2009. **652**(1): p. 161-172.
74. Lundstedt, T., et al., *Experimental design and optimization*. Chemometrics and intelligent laboratory systems, 1998. **42**(1-2): p. 3-40.
75. Plackett, R.L. and J.P. Burman, *The design of optimum multifactorial experiments*. Biometrika, 1946. **33**(4): p. 305-325.
76. Box, G.E. and D.W. Behnken, *Some new three level designs for the study of quantitative variables*. Technometrics, 1960. **2**(4): p. 455-475.
77. Prothmann, J., et al., *Ultra-high-performance supercritical fluid chromatography with quadrupole-time-of-flight mass spectrometry (UHPSFC/QTOF-MS) for analysis of lignin-derived monomeric compounds in processed lignin samples*. Analytical and Bioanalytical Chemistry, 2017. **409**(30): p. 7049-7061.
78. Weiss, R., et al., *Lignin-based pesticide delivery system*. ACS omega, 2020. **5**(8): p. 4322-4329.
79. Karlsson, M., et al., *Protected lignin biorefining through cyclic extraction: gaining fundamental insights into the tuneable properties of lignin by chemometrics*. Green Chemistry, 2022. **24**(3): p. 1211-1223.
80. Anderson, E.M., et al., *Reductive catalytic fractionation of corn stover lignin*. ACS Sustainable Chemistry & Engineering, 2016. **4**(12): p. 6940-6950.
81. Renders, T., et al., *Reductive catalytic fractionation: state of the art of the lignin-first biorefinery*. Current Opinion in Biotechnology, 2019. **56**: p. 193-201.
82. Deuss, P.J., K. Barta, and J.G. de Vries, *Homogeneous catalysis for the conversion of biomass and biomass-derived platform chemicals*. Catalysis Science & Technology, 2014. **4**(5): p. 1174-1196.
83. Gioia, C., et al., *Lignin-Based Epoxy Resins: Unravelling the Relationship between Structure and Material Properties*. Biomacromolecules, 2020. **21**(5): p. 1920-1928.

84. Jawerth, M.E., et al., *Mechanical and Morphological Properties of Lignin-Based Thermosets*. ACS Applied Polymer Materials, 2020. **2**(2): p. 668-676.
85. Roberts, D., *Methods in lignin chemistry*, ed. e.d.S.Y.L.a.C.W. Dence. 1992: Springer-Verlag.
86. Constant, S., et al., *New insights into the structure and composition of technical lignins: a comparative characterisation study*. Green Chemistry, 2016. **18**(9): p. 2651-2665.
87. Leppänen, K., et al., *Pressurized hot water extraction of Norway spruce hemicelluloses using a flow-through system*. Wood science and technology, 2011. **45**: p. 223-236.
88. Crestini, C., et al., *Milled wood lignin: a linear oligomer*. Biomacromolecules, 2011. **12**(11): p. 3928-3935.
89. Lancefield, C.S., et al., *Identification of a diagnostic structural motif reveals a new reaction intermediate and condensation pathway in kraft lignin formation*. Chemical Science, 2018. **9**(30): p. 6348-6360.
90. Capanema, E.A., M.Y. Balakshin, and J.F. Kadla, *A comprehensive approach for quantitative lignin characterization by NMR spectroscopy*. Journal of agricultural and food chemistry, 2004. **52**(7): p. 1850-1860.
91. Pu, Y., S. Cao, and A.J. Ragauskas, *Application of quantitative 31P NMR in biomass lignin and biofuel precursors characterization*. Energy & Environmental Science, 2011. **4**(9): p. 3154-3166.
92. Balakshin, M.Y., E.A. Capanema, and H.-m. Chang, *MWL fraction with a high concentration of lignin-carbohydrate linkages: Isolation and 2D NMR spectroscopic analysis*. 2007.
93. Archipov, Y., et al., *31P NMR spectroscopy in wood chemistry. I. Model compounds*. Journal of wood chemistry and technology, 1991. **11**(2): p. 137-157.
94. Zinovyev, G., et al., *Getting closer to absolute molar masses of technical lignins*. ChemSusChem, 2018. **11**(18): p. 3259-3268.
95. Ponnudurai, A., et al., *Fractionation and Absolute Molecular Weight Determination of Organosolv Lignin and Its Fractions: Analysis by a Novel Acetone-Based SEC— MALS Method*. ACS Sustainable Chemistry & Engineering, 2022.
96. Jacobs, A. and O. Dahlman, *Absolute molar mass of lignins by size exclusion chromatography and MALDI-TOF mass spectroscopy*. Nordic pulp & paper research journal, 2000. **15**(2): p. 120-127.
97. Metzger, J.O., et al., *Matrix-assisted laser desorption mass spectrometry of lignins*. Angewandte Chemie International Edition in English, 1992. **31**(6): p. 762-764.

98. Cameron, A. and D. Eggers Jr, *An Ion``Velocitron"*. Review of Scientific Instruments, 1948. **19**(9): p. 605-607.
99. Trimpin, S., H.J. Räder, and K. Müllen, *Investigations of theoretical principles for MALDI-MS derived from solvent-free sample preparation: Part I. Preorganization*. International Journal of Mass Spectrometry, 2006. **253**(1-2): p. 13-21.
100. Yoshioka, K., D. Ando, and T. Watanabe, *A Comparative Study of Matrix- and Nano-assisted Laser Desorption/Ionisation Time-of-Flight Mass Spectrometry of Isolated and Synthetic Lignin*. Phytochemical Analysis, 2012. **23**(3): p. 248-253.
101. Kosyakov, D.S., et al., *Ionic liquid matrices for MALDI mass spectrometry of lignin*. Analytical and Bioanalytical Chemistry, 2018. **410**(28): p. 7429-7439.
102. Letourneau, D.R. and D.A. Volmer, *Mass spectrometry-based methods for the advanced characterization and structural analysis of lignin: A review*. Mass Spectrom Rev, 2023. **42**(1): p. 144-188.
103. Qi, Y. and D.A. Volmer, *Chemical diversity of lignin degradation products revealed by matrix-optimized MALDI mass spectrometry*. Analytical and bioanalytical chemistry, 2019. **411**(23): p. 6031-6037.
104. Morreel, K., et al., *Mass Spectrometry-Based Sequencing of Lignin Oligomers*. Plant Physiology, 2010. **153**(4): p. 1464-1478.
105. Sheng, H., et al., *(−)ESI/CAD MSn Procedure for Sequencing Lignin Oligomers Based on a Study of Synthetic Model Compounds with β-O-4 and 5-5 Linkages*. Analytical Chemistry, 2017. **89**(24): p. 13089-13096.
106. Prothmann, J., et al., *Identification of lignin oligomers in Kraft lignin using ultra-high-performance liquid chromatography/high-resolution multiple-stage tandem mass spectrometry (UHPLC/HRMSn)*. Analytical and Bioanalytical Chemistry, 2018. **410**(29): p. 7803-7814.
107. Sun, M., M. Sandahl, and C. Turner, *Comprehensive on-line two-dimensional liquid chromatography × supercritical fluid chromatography with trapping column-assisted modulation for depolymerised lignin analysis*. Journal of Chromatography A, 2018. **1541**: p. 21-30.
108. Zhang, J., et al., *Compositional analysis of organosolv poplar lignin by using high-performance liquid chromatography/high-resolution multi-stage tandem mass spectrometry*. Green Chemistry, 2021. **23**(2): p. 983-1000.

109. Prothmann, J., et al., *Nontargeted Analysis Strategy for the Identification of Phenolic Compounds in Complex Technical Lignin Samples*. ChemSusChem, 2020. **13**(17): p. 4605-4612.
110. Lu, F. and J. Ralph, *Highly Selective Syntheses of Coniferyl and Sinapyl Alcohols*. Journal of Agricultural and Food Chemistry, 1998. **46**(5): p. 1794-1796.
111. Kim, H. and J. Ralph, *Simplified Preparation of Coniferyl and Sinapyl Alcohols*. Journal of Agricultural and Food Chemistry, 2005. **53**(9): p. 3693-3695.
112. Lancefield, C.S. and N.J. Westwood, *The synthesis and analysis of advanced lignin model polymers*. Green Chemistry, 2015. **17**(11): p. 4980-4990.
113. Karlsson, M., et al., *Lignin Structure and Reactivity in the Organosolv Process Studied by NMR Spectroscopy, Mass Spectrometry, and Density Functional Theory*. Biomacromolecules, 2023. DOI: 10.1021/acs.biomac.3c00186
114. Dababi, I., et al., *Organosolv lignin-based wood adhesive. Influence of the lignin extraction conditions on the adhesive performance*. Polymers, 2016. **8**(9): p. 340.
115. Li, J., G. Henriksson, and G. Gellerstedt, *Lignin depolymerization/repolymerization and its critical role for delignification of aspen wood by steam explosion*. Bioresource Technology, 2007. **98**(16): p. 3061-3068.
116. Sannigrahi, P., A.J. Ragauskas, and S.J. Miller, *Lignin structural modifications resulting from ethanol organosolv treatment of loblolly pine*. Energy & Fuels, 2010. **24**(1): p. 683-689.
117. McAvey, K.M., et al., *Laser-induced oxidation of cholesterol observed during MALDI-TOF mass spectrometry*. Journal of the American Society for Mass Spectrometry, 2011. **22**(4): p. 659-669.
118. Terashima, N., et al., *Proposed supramolecular structure of lignin in softwood tracheid compound middle lamella regions*. Holzforschung, 2012. **66**(8): p. 907-915.
119. Deng, Y., et al., *Investigation of aggregation and assembly of alkali lignin using iodine as a probe*. Biomacromolecules, 2011. **12**(4): p. 1116-1125.
120. Oliaei, E., et al., *Highly reinforced and degradable lignocellulose biocomposites by polymerization of new polyester oligomers*. Nature Communications, 2022. **13**(1): p. 5666.
121. Gan, D., et al., *Plant-inspired adhesive and tough hydrogel based on Ag-Lignin nanoparticles-triggered dynamic redox catechol chemistry*. Nature Communications, 2019. **10**(1): p. 1487.

122. Yang, W., et al., *Synergic effect of cellulose and lignin nanostructures in PLA based systems for food antibacterial packaging*. European Polymer Journal, 2016. **79**: p. 1-12.
123. Yang, W., et al., *Antioxidant and antibacterial lignin nanoparticles in polyvinyl alcohol/chitosan films for active packaging*. Industrial crops and products, 2016. **94**: p. 800-811.
124. Lee, S.C., et al., *Preparation and application of light-colored lignin nanoparticles for broad-spectrum sunscreens*. Polymers, 2020. **12**(3): p. 699.
125. Yearla, S.R. and K. Padmasree, *Preparation and characterisation of lignin nanoparticles: evaluation of their potential as antioxidants and UV protectants*. Journal of Experimental Nanoscience, 2016. **11**(4): p. 289-302.
126. Aravamuthan, R.G., *PULPING | Chemical Pulping*, in *Encyclopedia of Forest Sciences*, J. Burley, Editor. 2004, Elsevier: Oxford. p. 904-910.
127. Öhman, F., et al., *Method for separating lignin from black liquor. U.S. Patent 8,486,224, July 16, 2013*. (LignoBoost), US 8486224 B2, 2006.
128. Ma, M., et al., *A simple and effective approach to fabricate lignin nanoparticles with tunable sizes based on lignin fractionation*. Green Chemistry, 2020. **22**(6): p. 2011-2017.
129. Sipponen, M.H., et al., *Understanding Lignin Aggregation Processes. A Case Study: Budesonide Entrapment and Stimuli Controlled Release from Lignin Nanoparticles*. ACS Sustainable Chemistry & Engineering, 2018. **6**(7): p. 9342-9351.
130. Pylypchuk, I.V., et al., *New Insight into the Surface Structure of Lignin Nanoparticles Revealed by 1H Liquid-State NMR Spectroscopy*. ACS Sustainable Chemistry & Engineering, 2020. **8**(36): p. 13805-13812.